

A coupled focusing-defocusing complex short pulse equation: multisoliton, breather, and rogue wave

Jun Yang, Zuo-Nong Zhu *

School of Mathematical Sciences, Shanghai Jiao Tong University,
800 Dongchuan Road, Shanghai, 200240, P. R. China

Abstract

Nonlinear Schrödinger equation, short pulse equation and complex short pulse equation have important application in nonlinear optics. They can be derived from the Maxwell equation. In this paper, we investigate a coupled focusing-defocusing complex short pulse equation. The bright-bright, bright-dark and dark-dark soliton solutions of the coupled focusing-defocusing complex short pulse equation are given. Then the breathers are derived from the dark soliton solution. The rogue wave solutions are also constructed. The dynamics and the asymptotic behavior of the soliton solutions are analyzed, which reveals that there exist the elastic or inelastic collision in bright-bright soliton solution. But the interactions of bright-dark and dark-dark soliton solutions are both elastic.

Keywords: coupled focusing-defocusing complex short pulse equation, multisoliton, breather, rogue wave.

1 Introduction

As is well known, nonlinear Schrödinger(NLS) equation and the coupled NLS equation play an important role in nonlinear optics, plasma physics, water waves, and Bose-Einstein condensates [1–7]. However, in optical fibers, the NLS equation becomes less accurate to describe the propagation of ultra-short pulses because the width of optical pulse is in the order of femtosecond($10^{-15}s$) [8]. Schäfer and Wayne derived the short pulse (SP) equation [9]

$$u_{xt} = u + \frac{1}{6}(u^3)_{xx}, \quad (1)$$

which can describe the propagation of ultra-short optical pulses in nonlinear media. The short pulse equation is completely integrable [10, 11]. Connection between the short pulse equation and the sine-Gordon equation has been given by a hodograph transformation [12, 13]. Multi-soliton, multi-breather and rogue wave solutions for Eq.(1) have been constructed [14–16]. The geometric interpretation and integrable discretization of Eq.(1) have also been studied [17–19]. It has been revealed that there are great advantages of dealing with the complex short pulse(CSP) equation and complex multi-component short pulse equations which can more appropriately describe the propagation of optical pulse along the optical fibers [20–22]. The complex short pulse equation [20, 22] is

$$q_{xt} + q + \frac{1}{2}\sigma(|q|^2q_x)_x = 0, \quad (2)$$

*Corresponding author. Email: znzhu@sjtu.edu.cn

where $\sigma = \pm 1$ represents focusing- and defocusing-type. Its two-component form

$$\begin{aligned} q_{1,xt} + q_1 + \frac{1}{2}((|q_1|^2 + |q_2|^2)q_{1,x})_x &= 0, \\ q_{2,xt} + q_2 + \frac{1}{2}((|q_1|^2 + |q_2|^2)q_{2,x})_x &= 0, \end{aligned} \quad (3)$$

is first proposed by Feng [20]. It can be derived from the Maxwell equation [20]. The multi-bright-soliton, multi-breather and higher-order rogue wave solution of Eq.(2) for focusing case is derived in [20]. Meanwhile, the multi-dark-soliton of Eq.(2) for defocusing case is studied in [22]. For the two-component focusing-focusing case(3), the bright-bright and bright-dark soliton solutions are obtained [20, 23]. To the best of our knowledge, the focusing-defocusing case for the coupled complex short pulse equation has not been studied. In this paper, we investigate the following coupled focusing-defocusing complex short pulse equation:

$$\begin{aligned} q_{1,xt} + q_1 + \frac{1}{2}((\sigma_1|q_1|^2 + \sigma_2|q_2|^2)q_{1,x})_x &= 0, \\ q_{2,xt} + q_2 + \frac{1}{2}((\sigma_1|q_1|^2 + \sigma_2|q_2|^2)q_{2,x})_x &= 0, \end{aligned} \quad (4)$$

where $\sigma_1 = -\sigma_2 = 1$. The coupled focusing-defocusing complex short pulse equation was introduced by Feng [24]. Starting from the Lax pair of the coupled focusing-defocusing complex short pulse equation, we will construct its soliton solutions, including the bright-bright soliton, bright-dark soliton, dark-dark soliton, breather and rogue wave solutions. The asymptotic behaviors of two soliton solutions are studied. It will be shown that the coupled bright-bright soliton solution undergo fascinating interactions with redistribution of energy. We construct bright-dark soliton solution and dark-dark soliton solution. This means the bright-bright soliton and dark-dark soliton are supported simultaneously for the coupled focusing-defocusing complex short pulse equation. The collision of the two solitons are completely elastic behaviors. Furthermore, the breather solution is constructed and the rogue wave soliton solution is derived by resorting to the Taylor series expansion coefficients of the breather solutions.

2 Lax pairs and N-bright soliton solutions for the coupled focusing-defocusing complex short pulse equation

2.1 Lax pairs and bilinear form of Eq.(4)

The Lax pair for the coupled focusing-defocusing complex short pulse equation (4) is

$$\Psi_x = U\Psi, \quad \Psi_t = V\Psi, \quad (5)$$

with

$$U = \lambda \begin{pmatrix} I_2 & Q_x \\ R_x & -I_2 \end{pmatrix}, \quad V = \begin{pmatrix} -\frac{\lambda}{2}QR - \frac{1}{4\lambda}I_2 & -\frac{\lambda}{2}QRQ_x + \frac{1}{2}Q \\ -\frac{\lambda}{2}RQR_x - \frac{1}{2}R & \frac{\lambda}{2}QR + \frac{1}{4\lambda}I_2 \end{pmatrix},$$

where I_2 is a 2×2 identity matrix, Q , R are 2×2 matrices defined as

$$Q = \begin{pmatrix} q_1 & q_2 \\ q_2^* & q_1^* \end{pmatrix}, \quad R = \begin{pmatrix} q_1^* & -q_2 \\ -q_2^* & q_1 \end{pmatrix}.$$

Notice that

$$QR = RQ = (|q_1|^2 - |q_2|^2)I_2, \quad (6)$$

one can check that the compatibility condition $U_t - V_x + [U, V] = 0$ for (5) gives the coupled focusing-defocusing complex short pulse equation

$$\begin{aligned} q_{1,xt} + q_1 + \frac{1}{2}((|q_1|^2 - |q_2|^2)q_{1,x})_x &= 0, \\ q_{2,xt} + q_2 + \frac{1}{2}((|q_1|^2 - |q_2|^2)q_{2,x})_x &= 0. \end{aligned} \quad (7)$$

The coupled focusing-defocusing complex short pulse equation can be bilinearized as

$$\begin{aligned} D_s D_y g \cdot f &= gf, \\ D_s D_y h \cdot f &= hf, \\ D_s^2 f \cdot f &= \frac{1}{2}(|g|^2 - |h|^2), \end{aligned} \quad (8)$$

by dependent variable transformation

$$q_1 = \frac{g}{f}, \quad q_2 = \frac{h}{f}, \quad (9)$$

and the hodograph transformation

$$x = y - 2(\ln f)_s, \quad t = -s, \quad (10)$$

where

$$D_s^m D_y^n f \cdot g = (\partial_s - \partial_{s'})^m (\partial_y - \partial_{y'})^n f(y, s) \cdot g(y', s')|_{s'=s, y'=y}.$$

Proof: Dividing both sides by f^2 converts the bilinear equation(8) to

$$\left(\frac{g}{f}\right)_{sy} + 2\frac{g}{f}(\ln f)_{sy} = \frac{g}{f}, \quad (11)$$

$$\left(\frac{h}{f}\right)_{sy} + 2\frac{h}{f}(\ln f)_{sy} = \frac{h}{f}, \quad (12)$$

$$(\ln f)_{ss} = \frac{1}{4} \frac{(|g|^2 - |h|^2)}{f^2}. \quad (13)$$

From the dependent variable transformation and hodograph transformation, we have

$$\frac{\partial x}{\partial s} = -2(\ln f)_{ss} = -\frac{1}{2}(|q_1|^2 - |q_2|^2), \quad \frac{\partial x}{\partial y} = 1 - 2(\ln f)_{sy}, \quad (14)$$

which implies

$$\partial_y = \rho^{-1} \partial_x \quad \partial_s = -\partial_t - \frac{1}{2}(|q_1|^2 - |q_2|^2) \partial_x, \quad (15)$$

where $1 - 2(\ln f)_{sy} = \rho^{-1}$. The Eqs.(11) and (12) give

$$\begin{aligned} \partial_x \left(-\partial_t - \frac{1}{2}(|q_1|^2 - |q_2|^2) \partial_x\right) q_1 &= q_1, \\ \partial_x \left(-\partial_t - \frac{1}{2}(|q_1|^2 - |q_2|^2) \partial_x\right) q_2 &= q_2. \end{aligned} \quad (16)$$

2.2 N-bright soliton solution

N-soliton solution to the Eq.(7) can be expressed by the following pfaffians:

$$\begin{aligned} f &= (-1)^N \text{Pf}(a_1, \dots, a_{2N}, b_1, \dots, b_{2N}), \\ g &= (-1)^N \text{Pf}(d_0, \gamma_1, a_1, \dots, a_{2N}, b_1, \dots, b_{2N}), \\ h &= (-1)^N \text{Pf}(d_0, \gamma_2, a_1, \dots, a_{2N}, b_1, \dots, b_{2N}). \end{aligned} \quad (17)$$

The elements of the pfaffians are determined as

$$\begin{aligned}
\text{Pf}(a_j, a_k) &= \frac{p_j - p_k}{p_j + p_k} e^{\eta_j + \eta_k}, \quad \text{Pf}(a_j, b_k) = \delta_{j,k} \\
\text{Pf}(b_j, b_k) &= \frac{1}{4} \frac{\alpha_j \alpha_k - \beta_j \beta_k}{p_j^{-2} - p_k^{-2}} \delta_{\mu+1, \nu}, \quad \text{Pf}(d_l, a_k) = p_k^l e^{\eta_k} \\
\text{Pf}(b_j, \gamma_1) &= \alpha_j \delta_{\mu, i}, \quad \text{Pf}(b_j, \gamma_2) = \beta_j \delta_{\mu, i}, \\
\text{Pf}(d_0, b_j) &= \text{Pf}(d_0, \gamma_1) = \text{Pf}(d_0, \rho_i) = \text{Pf}(a_j, \gamma_2) = \text{Pf}(a_j, \gamma_i) = 0.
\end{aligned} \tag{18}$$

Here we need to define two sets: $B_\mu (\mu = 1, 2) : B_1 = \{b_1, b_2, \dots, b_N\}, B_2 = \{b_{N+1}, b_{N+2}, \dots, b_{2N}\}$ and an index function of b_j by $\text{index}(b_j) = \mu$ if $b_j \in B_\mu$. $\mu = \text{index}(b_j)$, $\nu = \text{index}(b_k)$, $\eta_j = p_j y + p_j^{-1} s + \eta_{j,0}$, which satisfy $p_{j+N} = \bar{p}_j$, $\alpha_{j+N} = \bar{\alpha}_j$, $\beta_{j+N} = \bar{\beta}_j$, where \bar{p}_j , $\bar{\alpha}_j$ and $\bar{\beta}_j$ represent the complex conjugates of p_j , α_j and β_j .

The proof of the N-soliton solution is similar to the ones of the coupled focusing-focusing complex short pulse equation with γ_j substituting $\beta_j (j = 1, 2)$ in appendix (A.9) [23] except the following formula

$$\begin{aligned}
\frac{1}{2}(g_1 g_1^* - g_2 g_2^*) &= \frac{1}{2} \sum_{i,j}^{2N} (-1)^{i+j} \text{Pf}(b_i, \gamma_1) \text{Pf}(d_0, \dots, \hat{b}_i, \dots) \times \text{Pf}(b_j, \gamma_1^*) \text{Pf}(d_0, \dots, \hat{b}_j, \dots) \\
&\quad - \frac{1}{2} \sum_{i,j}^{2N} (-1)^{i+j} \text{Pf}(b_i, \gamma_2) \text{Pf}(d_0, \dots, \hat{b}_i, \dots) \times \text{Pf}(b_j, \gamma_2^*) \text{Pf}(d_0, \dots, \hat{b}_j, \dots) \\
&= \frac{1}{4} \sum_{i,j}^{2N} (-1)^{i+j} \alpha_i \alpha_j^* \times \text{Pf}(d_0, \dots, \hat{b}_i, \dots) \text{Pf}(d_0, \dots, \hat{b}_j, \dots) \\
&\quad - \frac{1}{4} \sum_{i,j}^{2N} (-1)^{i+j} \beta_i \beta_j^* \times \text{Pf}(d_0, \dots, \hat{b}_i, \dots) \text{Pf}(d_0, \dots, \hat{b}_j, \dots) \\
&= \frac{1}{4} \sum_{i,j}^{2N} (-1)^{i+j} (\alpha_i \alpha_j^* - \beta_i \beta_j^*) \times \text{Pf}(d_0, \dots, \hat{b}_i, \dots) \text{Pf}(d_0, \dots, \hat{b}_j, \dots) \\
&= \frac{1}{2} \sum_{i,j}^{2N} (-1)^{i+j} (p_i^{-2} - p_j^{-2}) \times \text{Pf}(b_i, b_j) \text{Pf}(d_0, \dots, \hat{b}_i, \dots) \text{Pf}(d_0, \dots, \hat{b}_j, \dots).
\end{aligned}$$

We can see that $q_1 = \frac{g}{f}$, $q_2 = \frac{h}{f}$ is the N-bright soliton solutions to the Eq.(7) under the hodograph transformation (10), where f, g, h are described by Eq.(17).

2.2.2 One soliton solution

Based on (17), one-soliton solution $q_1 = \frac{g}{f}$, $q_2 = \frac{h}{f}$ is given by

$$f = 1 + \frac{1}{4} \frac{(|\alpha_1|^2 - |\beta_1|^2) |p_1|^4}{(p_1 + p_1^*)^2} e^{\eta_1 + \eta_1^*}, \tag{19}$$

$$g = \alpha_1 e^{\eta_1}, h = \beta_1 e^{\eta_1}. \tag{20}$$

In order to obtain the bright soliton, the condition $|\alpha_1| > |\beta_1|$ needs to be satisfied. Let $p_1 = p_{1R} + ip_{1I}$ and

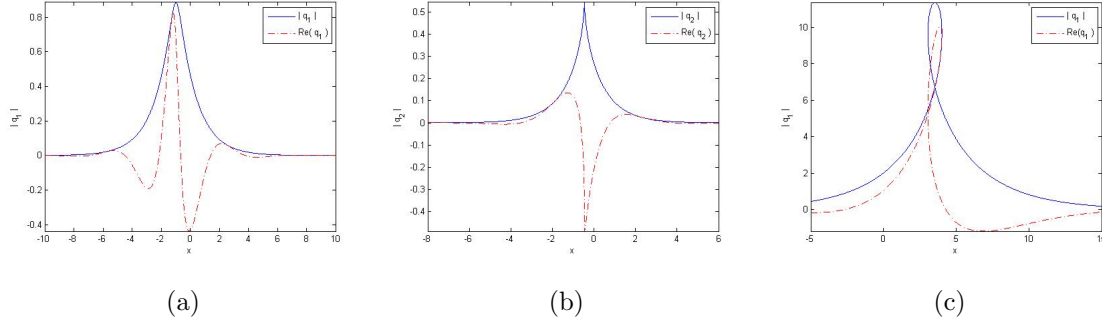


Fig. 1: One bright soliton to the coupled focusing-defocusing complex short pulse equation: (a)-(c) profiles with solid line $|q|$ and dashed line $Re(q)$ at $t = 0$. (a) smooth soliton with $p_1 = 0.8 + 1.3i$, $\alpha_1 = 1 + 2i$, $\beta_1 = 1 - i$, (b) cuspon soliton with $p_1 = 1 + i$, $\alpha_1 = 2 - 3i$, $\beta_1 = 1 + 1.4i$, (c) loop soliton with $p_1 = 2 - i$, $\alpha_1 = 1 + 1.7i$, $\beta_1 = 1 - 1.5i$.

assume $p_{1R} > 0$ then the one-soliton solution is

$$\begin{pmatrix} q_1 \\ q_2 \end{pmatrix} = \begin{pmatrix} A_1 \\ A_2 \end{pmatrix} \frac{2p_{1R}}{|p_1|^2} e^{i\eta_{1I}} \text{sech}(\eta_{1R} + \eta_{10}), \quad (21)$$

$$x = y - 2 \frac{p_{1R}}{|p_1|^2} (1 + \tanh(\eta_{1R} + \eta_{10})), \quad t = -s,$$

where

$$\begin{aligned} \eta_{1R} &= p_{1R}y + \frac{p_{1R}}{|p_1|^2}s + \eta_{1,0R}, & \eta_{1I} &= p_{1I}y - \frac{p_{1I}}{|p_1|^2}s + \eta_{1,0I}, \\ A_1 &= \frac{\alpha_1}{\sqrt{|\alpha_1|^2 - |\beta_1|^2}}, & A_2 &= \frac{\beta_1}{\sqrt{|\alpha_1|^2 - |\beta_1|^2}}, & \eta_{10} &= \ln \frac{\sqrt{|\alpha_1|^2 - |\beta_1|^2} |p_1|^2}{4|p_{1R}|}. \end{aligned} \quad (22)$$

Eq. (21) is an envelope bright soliton with the amplitude $2|A_j|p_{1R}/|p_1|^2$ ($j = 1, 2$), velocity $-\frac{1}{|p_1|^2}$ and phase η_{10} . Let us analyze the property for the one-soliton solution. Notice that

$$\frac{\partial x}{\partial y} = 1 - \frac{2p_{1R}^2}{|p_1|^2} \text{sech}^2(\eta_{1R} + \eta_{10}), \quad (23)$$

We have $\frac{\partial x}{\partial y} \rightarrow 1$ as $y \rightarrow \pm\infty$. The term $\frac{\partial x}{\partial y}$ attains a minimum value $(p_{1I}^2 - p_{1R}^2)/(p_{1I}^2 + p_{1R}^2)$ at the peak point of soliton wave. Since $\frac{\partial|q_j|}{\partial x} = \frac{\partial|q_j|}{\partial y} / \frac{\partial x}{\partial y}$, we classify the one-soliton solution as follows:

- smooth soliton: when $|p_{1R}| < |p_{1I}|$, $\frac{\partial x}{\partial y}$ is always positive, which leads to a smooth envelope soliton. An example with $p_1 = 0.8 + 1.3i$ is illustrated in Fig. 1(a).
- cuspon soliton: when $|p_{1R}| = |p_{1I}|$, $\frac{\partial x}{\partial y}$ has a minimum value of zero at $\eta_{1R} + \eta_{10} = 0$, which makes the derivative of the envelope $|q_j|$ with respect to x going to infinity at the peak point. Thus, we have a cusponed envelope soliton, which is illustrated in Fig. 1(b) with $p_1 = 1 + i$.
- loop soliton: when $|p_{1R}| > |p_{1I}|$, the minimum value of $\frac{\partial x}{\partial y}$ becomes negative and $\frac{\partial x}{\partial y}$ has two zeros at both sides of the peak of the envelope soliton. This leads to a loop soliton for the envelope of q_j . An example is shown in Fig. 1(c) with $p_1 = 0.38 - 0.21i$.

2.2.3 bright-bright soliton solution

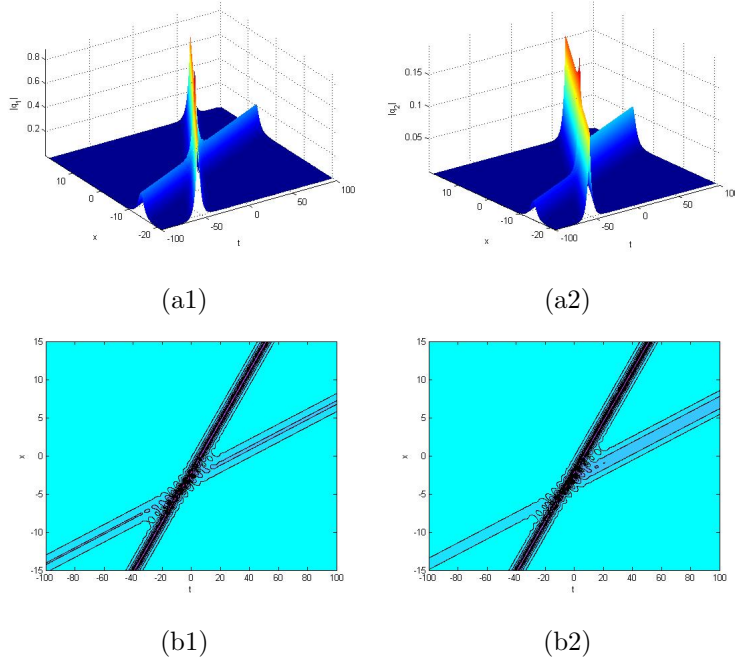


Fig. 2: (a1)-(a2) describe inelastic collision and energy exchange between two bright-bright soliton solutions to coupled focusing-defocusing complex short pulse equation. (b1)-(b2) are contour plots.

From the N-soliton solution expression (17)-(18) of the coupled focusing-defocusing complex short pulse equation, we obtain two-soliton solution $q_1 = \frac{g}{f}$, $q_2 = \frac{h}{f}$, where

$$\begin{aligned}
f &= \text{Pf}(a_1, a_2, a_3, a_4, b_1, b_2, b_3, b_4) \\
&= 1 + e^{\eta_1 + \bar{\eta}_1 + \theta_{1\bar{1}}} + e^{\eta_1 + \bar{\eta}_2 + \theta_{1\bar{2}}} + e^{\eta_2 + \bar{\eta}_1 + \theta_{2\bar{1}}} + e^{\eta_2 + \bar{\eta}_2 + \theta_{2\bar{2}}} \\
&\quad + |P_{12}|^2 |P_{1\bar{2}}|^2 P_{1\bar{1}} P_{2\bar{2}} (B_{1\bar{1}} B_{2\bar{2}} - B_{2\bar{1}} B_{1\bar{2}}) e^{\eta_1 + \eta_2 + \bar{\eta}_1 + \bar{\eta}_2},
\end{aligned} \tag{24}$$

$$\begin{aligned}
g &= \text{Pf}(d_0, \gamma_1, a_1, a_2, a_3, a_4, b_1, b_2, b_3, b_4) \\
&= \alpha_1 e^{\eta_1} + \alpha_2 e^{\eta_2} + P_{12} P_{1\bar{1}} P_{2\bar{1}} (\alpha_2 B_{1\bar{1}} - \alpha_1 B_{2\bar{1}}) e^{\eta_1 + \eta_2 + \bar{\eta}_1} \\
&\quad + P_{12} P_{1\bar{2}} P_{2\bar{2}} (\alpha_2 B_{1\bar{2}} - \alpha_1 B_{2\bar{2}}) e^{\eta_1 + \eta_2 + \bar{\eta}_2},
\end{aligned} \tag{25}$$

$$\begin{aligned}
h &= \text{Pf}(d_0, \gamma_2, a_1, a_2, a_3, a_4, b_1, b_2, b_3, b_4) \\
&= \beta_1 e^{\eta_1} + \beta_2 e^{\eta_2} + P_{12} P_{1\bar{1}} P_{2\bar{1}} (\beta_2 B_{1\bar{1}} - \beta_1 B_{2\bar{1}}) e^{\eta_1 + \eta_2 + \bar{\eta}_1} \\
&\quad + P_{12} P_{1\bar{2}} P_{2\bar{2}} (\beta_2 B_{1\bar{2}} - \beta_1 B_{2\bar{2}}) e^{\eta_1 + \eta_2 + \bar{\eta}_2},
\end{aligned} \tag{26}$$

where

$$P_{ij} = \frac{p_i - p_j}{p_i + p_j}, P_{i\bar{j}} = \frac{p_i - \bar{p}_j}{p_i + \bar{p}_j}, B_{i\bar{j}} = \frac{\alpha_i \bar{\alpha}_j - \beta_i \bar{\beta}_j}{4(p_i^{-2} - \bar{p}_j^{-2})}, e^{\theta_{i\bar{j}}} = \frac{\alpha_i \bar{\alpha}_j - \beta_i \bar{\beta}_j}{4(p_i^{-1} + \bar{p}_j^{-1})^2}. \tag{27}$$

Remark 1: In order to obtain bright-bright solitons, the conditions $|\alpha_j| > |\beta_j| (j = 1, 2)$ still need to be satisfied. From the forward analysis, we know that the condition $|p_{jR}| < |p_{jI}|$, $|p_{jR}| = |p_{jI}|$, $|p_{jR}| > |p_{jI}|$ leads to

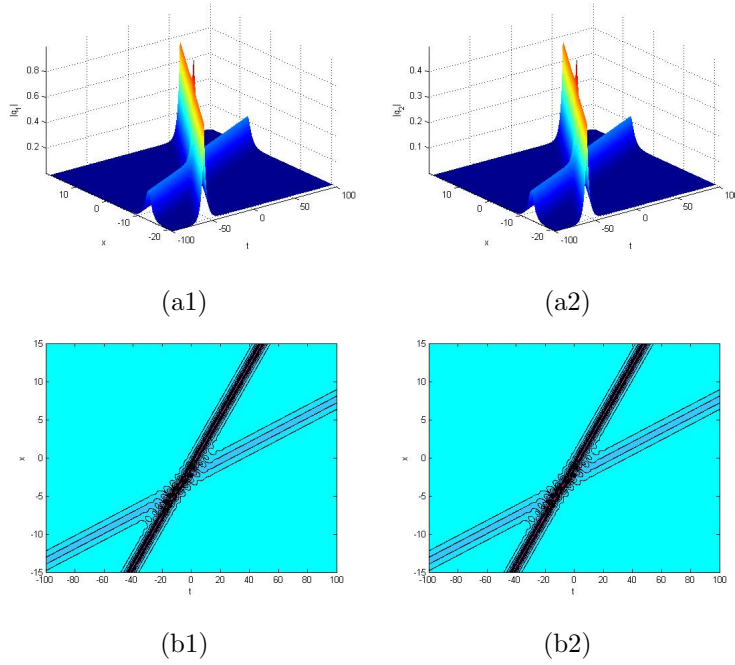


Fig. 3: (a1)-(a2) describe elastic collision in coupled focusing-defocusing complex short pulse equation. (b1)-(b2) are contour plots.

the smooth soliton, the cuspon soliton and the loop soliton, respectively. Next, we investigate the asymptotic behavior of the bright-bright soliton solutions (24)-(26) under the reciprocal transformation(10). We assume $p_{1R}, p_{2R} > 0$, $|p_2| > |p_1|$ without loss of generality. We discuss the following two cases: (i) when the wave- η_{1R} is fixed, η_{2R} can be written as $\eta_{2R} = \frac{p_{2R}}{p_{1R}}\eta_{1R} + p_{2R}\left(\frac{1}{|p_2|^2} - \frac{1}{|p_1|^2}\right)s$. When $t \rightarrow \pm\infty$, $\eta_{2R} \rightarrow \pm\infty$ for soliton 1. (ii) the wave- η_{2R} is fixed, η_{1R} can be written as $\eta_{1R} = \frac{p_{1R}}{p_{2R}}\eta_{2R} + p_{1R}\left(\frac{1}{|p_1|^2} - \frac{1}{|p_2|^2}\right)s$. When $t \rightarrow \pm\infty$, $\eta_{1R} \rightarrow \mp\infty$ for soliton 2. This leads to the following asymptotic forms for two-soliton solution.

(i) Before collision ($t \rightarrow -\infty$):

Soliton 1(the wave- η_{1R} is fixed, $\eta_{2R} \rightarrow -\infty$),

$$\begin{aligned} \begin{pmatrix} q_1 \\ q_2 \end{pmatrix} &\rightarrow \begin{pmatrix} \alpha_1 \\ \beta_1 \end{pmatrix} \frac{e^{\eta_1}}{1 + e^{\eta_1 + \eta_1^* + \theta_{11}}} \\ &= \begin{pmatrix} A_1^{1-} \\ A_2^{1-} \end{pmatrix} \frac{2p_{1R}}{|p_1|^2} e^{i\eta_{1I}} \operatorname{sech}\left(\eta_{1R} + \frac{\theta_{11}}{2}\right), \end{aligned} \quad (28)$$

where

$$\begin{pmatrix} A_1^{1-} \\ A_2^{1-} \end{pmatrix} = \begin{pmatrix} \alpha_1 \\ \beta_1 \end{pmatrix} \frac{1}{\sqrt{|\alpha_1|^2 - |\beta_1|^2}}. \quad (29)$$

Soliton 2(the wave- η_{2R} is fixed, $\eta_{1R} \rightarrow +\infty$),

$$\begin{pmatrix} q_1 \\ q_2 \end{pmatrix} \rightarrow \begin{pmatrix} A_1^{2-} \\ A_2^{2-} \end{pmatrix} \frac{2p_{2R}}{|p_2|^2} e^{i\eta_{2I}} \operatorname{sech}\left(\eta_{2R} + \frac{\theta_{11\bar{2}\bar{2}} - \theta_{11\bar{1}}}{2}\right), \quad (30)$$

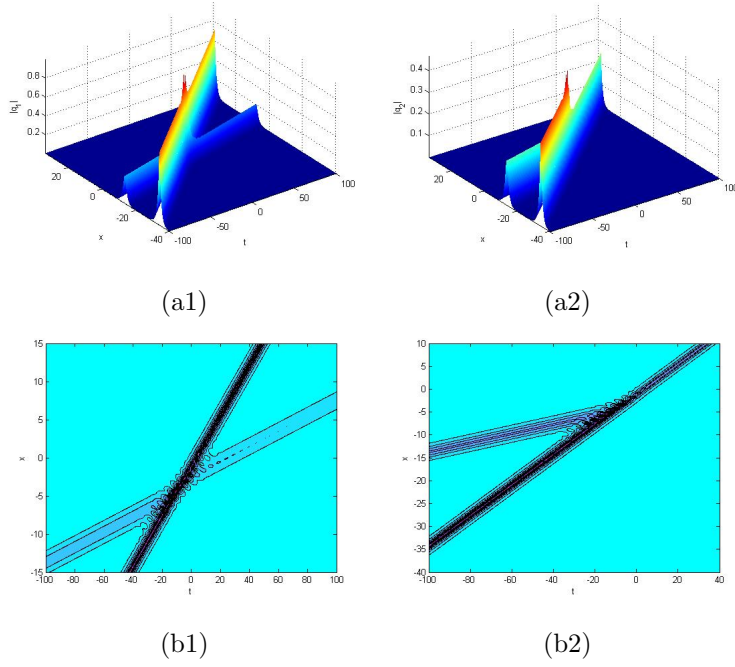


Fig. 4: (a1)-(a2) describe inelastic collision in coupled focusing-defocusing complex short pulse equation for $p_1 = 1 - \sqrt{2}i$, $p_2 = 1 + 3i$, $\alpha_1 = 3$, $\alpha_2 = 2$, $\beta_1 = 1$, $\beta_2 = 0$. (b1)-(b2) are contour plots.

where

$$\begin{pmatrix} A_1^{2-} \\ A_2^{2-} \end{pmatrix} = \begin{pmatrix} e^{\theta_{12\bar{1}}^{(1)}} \\ e^{\theta_{12\bar{1}}^{(2)}} \end{pmatrix} \frac{e^{-(\theta_{1\bar{1}2\bar{2}} + \theta_{1\bar{1}} - \theta_{2\bar{2}})/2}}{\sqrt{|\alpha_2|^2 - |\beta_2|^2}}, \quad (31)$$

with

$$\begin{aligned} \theta_{12\bar{1}}^{(1)} &= P_{12}P_{1\bar{1}}P_{2\bar{1}}(\alpha_2 B_{1\bar{1}} - \alpha_1 B_{2\bar{1}}), \\ \theta_{12\bar{1}}^{(2)} &= P_{12}P_{1\bar{1}}P_{2\bar{1}}(\beta_2 B_{1\bar{1}} - \beta_1 B_{2\bar{1}}), \\ \theta_{1\bar{1}2\bar{2}} &= P_{12}P_{1\bar{2}}P_{2\bar{2}}(\alpha_2 B_{1\bar{2}} - \alpha_1 B_{2\bar{2}}). \end{aligned}$$

(ii) After collision ($t \rightarrow +\infty$):

Soliton 1 (the wave- η_{1R} is fixed, $\eta_{2R} \rightarrow +\infty$),

$$\begin{pmatrix} q_1 \\ q_2 \end{pmatrix} \rightarrow \begin{pmatrix} A_1^{1+} \\ A_2^{1+} \end{pmatrix} \frac{2p_{1R}}{|p_1|^2} e^{i\eta_{1I}} \operatorname{sech}\left(\eta_{1R} + \frac{\theta_{1\bar{1}2\bar{2}} - \theta_{2\bar{2}}}{2}\right), \quad (32)$$

where

$$\begin{pmatrix} A_1^{1+} \\ A_2^{1+} \end{pmatrix} = \begin{pmatrix} e^{\theta_{122}^{(1)}} \\ e^{\theta_{122}^{(2)}} \end{pmatrix} \frac{e^{-(\theta_{1\bar{1}2\bar{2}} + \theta_{2\bar{2}} - \theta_{1\bar{1}})/2}}{\sqrt{|\alpha_1|^2 - |\beta_1|^2}}, \quad (33)$$

with

$$\begin{aligned} \theta_{122}^{(1)} &= P_{12}P_{12}P_{2\bar{2}}(\alpha_2 B_{12} - \alpha_1 B_{2\bar{2}}), \\ \theta_{122}^{(2)} &= P_{12}P_{12}P_{2\bar{2}}(\beta_2 B_{12} - \beta_1 B_{2\bar{2}}). \end{aligned}$$

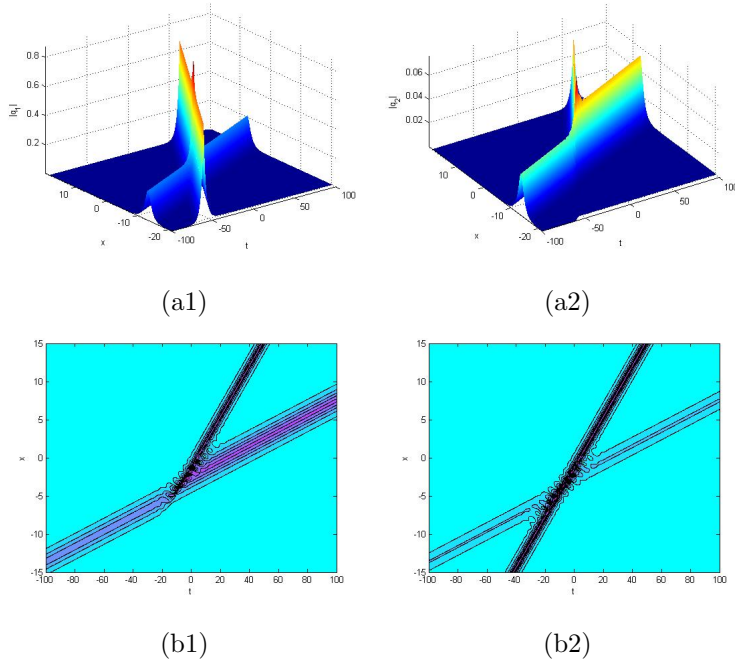


Fig. 5: (a1)-(a2) describe inelastic collision in coupled focusing-defocusing complex short pulse equation for $p_1 = 1 - \sqrt{2}i, p_2 = 1 + 3i, \alpha_1 = 3, \alpha_2 = 2, \beta_1 = 0, \beta_2 = 1$. (b1)-(b2) are contour plots.

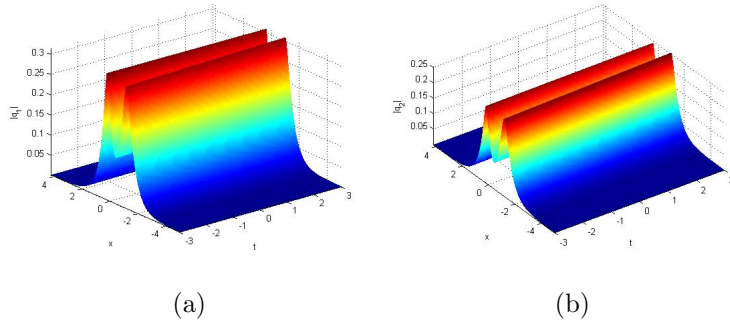


Fig. 6: Parallel two bright-bright solitons in coupled focusing-defocusing complex short pulse equation for $p_1 = 3 + 4i, p_2 = 2 + \sqrt{2}i, \alpha_1 = 2, \alpha_2 = 3, \beta_1 = 1.6, \beta_2 = 2.5$.

Soliton 2:(the wave- η_{2R} is fixed, $\eta_{1R} \rightarrow -\infty$),

$$\begin{pmatrix} q_1 \\ q_2 \end{pmatrix} \rightarrow \begin{pmatrix} A_1^{2+} \\ A_2^{2+} \end{pmatrix} \frac{2p_{2R}}{|p_2|^2} e^{i\eta_{2I}} \operatorname{sech}\left(\eta_{2R} + \frac{\theta_{2\bar{2}}}{2}\right),$$

where

$$\begin{pmatrix} A_1^{2+} \\ A_2^{2+} \end{pmatrix} = \begin{pmatrix} \alpha_2 \\ \beta_2 \end{pmatrix} \frac{1}{\sqrt{|\alpha_2|^2 - |\beta_2|^2}}. \quad (34)$$

Table 1: Physical quantities of bright-bright soliton S_1 and soliton S_2 before and after interactions.

Soliton	Amplitude/depth	Velocity	Soliton	Amplitude/depth	Velocity
S_1^{1-}	$\frac{2\alpha_1 p_{1R}}{ p_1 ^2 \sqrt{ \alpha_1 ^2 - \beta_1 ^2}}$	$-\frac{1}{ p_1 ^2}$	S_1^{1+}	$\frac{2p_{1R} e^{\theta_{122}^{(1)} - (\theta_{1122} + \theta_{22} - \theta_{11})/2}}{ p_1 ^2 \sqrt{ \alpha_1 ^2 - \beta_1 ^2}}$	$-\frac{1}{ p_1 ^2}$
S_2^{1-}	$\frac{2\beta_1 p_{1R}}{ p_1 ^2 \sqrt{ \alpha_1 ^2 - \beta_1 ^2}}$	$-\frac{1}{ p_1 ^2}$	S_2^{1+}	$\frac{2p_{1R} e^{\theta_{122}^{(2)} - (\theta_{1122} + \theta_{22} - \theta_{11})/2}}{ p_1 ^2 \sqrt{ \alpha_1 ^2 - \beta_1 ^2}}$	$-\frac{1}{ p_1 ^2}$
S_1^{2-}	$\frac{2p_{2R} e^{\theta_{121}^{(1)} - (\theta_{1122} + \theta_{11} - \theta_{22})/2}}{ p_2 ^2 \sqrt{ \alpha_2 ^2 - \beta_2 ^2}}$	$-\frac{1}{ p_2 ^2}$	S_1^{2+}	$\frac{2\alpha_2 p_{2R}}{ p_2 ^2 \sqrt{ \alpha_2 ^2 - \beta_2 ^2}}$	$-\frac{1}{ p_2 ^2}$
S_2^{2-}	$\frac{2p_{2R} e^{\theta_{121}^{(2)} - (\theta_{1122} + \theta_{11} - \theta_{22})/2}}{ p_2 ^2 \sqrt{ \alpha_2 ^2 - \beta_2 ^2}}$	$-\frac{1}{ p_2 ^2}$	S_2^{2+}	$\frac{2\beta_2 p_{2R}}{ p_2 ^2 \sqrt{ \alpha_2 ^2 - \beta_2 ^2}}$	$-\frac{1}{ p_2 ^2}$

Similar to the analysis of the coupled focusing-focusing complex short pulse equation [20] and the coupled focusing-focusing NLS equation [26–28], we introduce the transition matrix $T = [T_j^l]$ defined by $A_j^{l+} = T_j^l A_j^{l-}$ ($j, l = 1, 2$), and set $\gamma_1 = \frac{\alpha_2}{\alpha_1}$, $\gamma_2 = \frac{\beta_2}{\beta_1}$. Then we have

$$T_j^1 = -\frac{P_{12} P_{1\bar{2}}}{|P_{12} P_{1\bar{2}}|} \frac{1}{\sqrt{1 - \lambda_1 \lambda_2}} (1 - \lambda_2 \gamma_j),$$

$$T_j^2 = \left(\frac{P_{12} P_{2\bar{1}}}{|P_{12} P_{2\bar{1}}|} \right)^{-1} \sqrt{1 - \lambda_1 \lambda_2} (1 - \lambda_1 \gamma_j^{-1})^{-1} \quad (j = 1, 2),$$

where $\lambda_1 = B_{2\bar{1}}/B_{1\bar{1}}$, $\lambda_2 = B_{1\bar{2}}/B_{2\bar{2}}$.

From the above analysis, we can see that there exist an exchange of energies between the two solitons after the collision. An example is shown in Fig.2 for the parameters $p_1 = 1 - \sqrt{2}i$, $p_2 = 1 + 3i$, $\alpha_1 = 5$, $\alpha_2 = 7$, $\beta_1 = 1$, $\beta_2 = 2$. However, only for the special case $\alpha_1/\alpha_2 = \beta_1/\beta_2$ there is no energy exchange between two components of solitons after the collision. An example is shown in Fig.3 for the parameters $p_1 = 1 - \sqrt{2}i$, $p_2 = 1 + 3i$, $\alpha_1 = 2$, $\alpha_2 = 4$, $\beta_1 = 1$, $\beta_2 = 2$.

Fig.4 and Fig.5 show the energy centralization and distribution between the two solitons q_1 and q_2 in the process of collision respectively. We just change the parameters in previous two examples as $\beta_1 = 0$, $\beta_2 = 1$ for Fig.4 and $\beta_1 = 1$, $\beta_2 = 0$ for Fig.5. When $|p_1| = |p_2|$, the parallel solitons will occur (see Fig. 6).

3 Bright-dark soliton and dark-dark soliton

3.1 bright-dark soliton solution

In order to obtain bright-dark soliton, we bilinearize the equation (7) as

$$D_s D_y f \cdot g = f \cdot g,$$

$$(D_s D_y - \lambda) f \cdot h = 0, \tag{35}$$

$$(D_s^2 - \lambda) f \cdot f = \frac{1}{2} (|g|^2 - |h|^2),$$

where λ is a constant to be determined. By the similar procedure of obtaining Eqs.(8)-(16), one can check that the bilinear form (35) can convert to the Eq.(7) by the following hodograph transformation

$$x = \lambda(y + s) - 2(\ln f)_s, \quad t = -s. \tag{36}$$

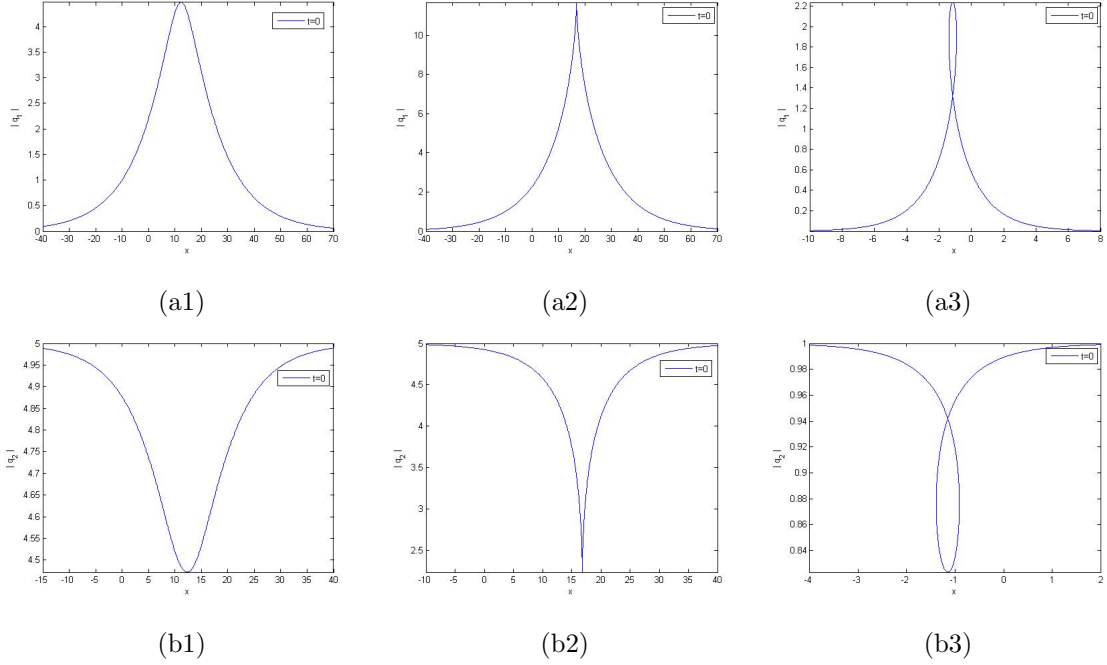


Fig. 7: One bright and dark soliton solution of q_1 and q_2 respectively to the coupled focusing-defocusing complex short pulse equation with parameters $k = 1, \tau_1 = 5, a_1 = 1 + 2i, b_1 = 0$. (a1)-(b1) smooth soliton with $p_1 = 1 + 2i$. (a2)-(b2) cuspon soliton with $p_1 = 1 + i$, (a3)-(b3) loop soliton with $\tau_1 = 1, p_1 = 0.3 - 0.2i$.

To get the bright-dark soliton solution, we assume $g = \chi g_1$, $h = h_0(1 + \chi^2 h_2)$, and $f = 1 + \chi^2 f_2$. Substituting them to the bilinear equation (35) and comparing the coefficient of the same power of χ^0, χ^1 , we get

$$h_0 = \tau_1 e^{i\psi}, \quad g_1 = a_1 e^{\eta_1},$$

where $\psi = ky - \frac{\lambda}{k}s$, $\eta_1 = p_1 y + \frac{\lambda}{p_1}s + b_1$, $\lambda = \frac{1}{2}|\tau_1|^2$, and here k is an arbitrary real parameter, τ_1, a_1, p_1, b_1 are arbitrary complex parameters. Substituting the form of h_0 into (35) then the bilinear equations change into

$$\begin{aligned} D_s D_y f \cdot g &= f \cdot g, \\ (D_s D_y - ik D_s + \frac{i\lambda}{k} D_y) f \cdot \tilde{h} &= 0, \\ (D_s^2 - \lambda) f \cdot f &= \frac{1}{2}(|g|^2 - \tau_1^2 |\tilde{h}|^2), \end{aligned} \quad (37)$$

where $\tilde{h} = 1 + \chi^2 h_2$. We set $h_2 = A_{1\bar{1}} e^{\eta_1 + \eta_1^*}, f_2 = B_{1\bar{1}} e^{\eta_1 + \eta_1^*}$, $\eta_1 = \eta_{1R} + i\eta_{1I}$ and $p_1 = p_{1R} + ip_{1I}$. This yields the bright-dark soliton solution

$$\begin{aligned} q_1 &= \frac{a_1 e^{\eta_1}}{1 + B_{1\bar{1}} e^{\eta_1 + \eta_1^*}} = \frac{a_1}{2} e^{i\eta_{1I} - \eta_{10}} \operatorname{sech}(\eta_{1R} + \eta_{10}), \\ q_2 &= \tau_1 e^{i\psi} \frac{1 + A_{1\bar{1}} e^{\eta_1 + \eta_1^*}}{1 + B_{1\bar{1}} e^{\eta_1 + \eta_1^*}} = \frac{1}{2} \tau_1 e^{i\psi} [1 + \mu_{1\bar{1}} - (1 - \mu_{1\bar{1}}) \tanh(\eta_{1R} + \eta_{10})], \\ x &= \lambda(y + s - 2 \frac{p_{1R}}{|p_1|^2} (\tanh(\eta_{1R} + \eta_{10}) + 1)), \quad t = -s, \end{aligned} \quad (38)$$

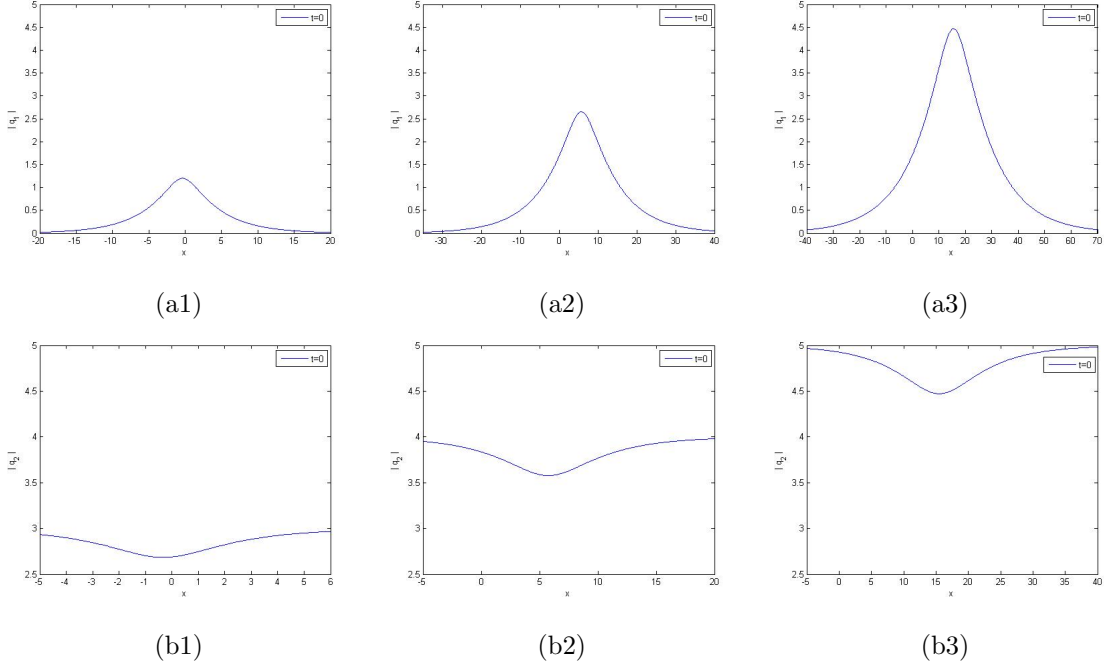


Fig. 8: Intensity plots of one-soliton of the coupled focusing-defocusing complex short pulse equation for different values of the background parameter τ_1 for the fixed values of $k = 1$, $a_1 = 1 + \sqrt{2}i$, $p_1 = 1 + 2i$, $b_1 = 0$. Note that the intensity of the bright soliton increases as the depth of the dark soliton decreases. The other parameters are chosen as $b_1 = 0$, $\tau_1 = 3, 4, 5$ respectively.

where

$$\begin{aligned} \eta_{1R} &= p_{1R}y + \frac{\lambda p_{1R}}{|p_1|^2}s + b_{1R}, \quad \eta_{1I} = p_{1I}y - \frac{\lambda p_{1I}}{|p_1|^2}s + b_{1I}, \quad \eta_{10} = \frac{1}{2} \ln B_{1\bar{1}}, \\ B_{1\bar{1}} &= \frac{|a_1|^2 |p_1|^4 (k^2 + p_1^2)(k^2 + p_1^{*2})}{4\lambda(p_1 + p_1^*)^2 [\lambda k^2 (k^2 + p_1^2 + p_1^{*2}) + |p_1|^4 (\lambda - 2k^2)]}, \\ \mu_{1\bar{1}} &= \frac{(k + ip_1)(k + ip_1^*)}{(k - ip_1)(k - ip_1^*)}, \quad A_{1\bar{1}} = \mu_{1\bar{1}} B_{1\bar{1}}. \end{aligned}$$

In order to avoid singularity, we emphasize $B_{1\bar{1}} > 0$, which means

$$|\tau_1| > \frac{2|kp_1|^2}{|p_1^2 + k^2|}. \quad (39)$$

Notice that

$$\frac{\partial x}{\partial y} = \lambda - \frac{2\lambda p_{1R}^2}{|p_1|^2} \operatorname{sech}^2(\eta_{1R} + \eta_{10}), \quad (40)$$

we have $\frac{\partial x}{\partial y} \rightarrow \lambda$ as $y \rightarrow \pm\infty$. Since $\partial|q_i|/\partial x = \frac{\partial|q_i|/\partial y}{\partial x/\partial y}$, we can also classify the one-soliton solution as smooth, cuspon and loop soliton respectively when $|p_{1R}| < |p_{1I}|$, $|p_{1R}| = |p_{1I}|$ and $|p_{1R}| > |p_{1I}|$. An example is shown in Fig. 7. The amplitude of the bright soliton is $\frac{\alpha_1}{2\sqrt{B_{1\bar{1}}}}$ with the velocity $-\frac{\lambda p_{1R}}{|p_1|^2}$ in the (y,s) -coordinate system and

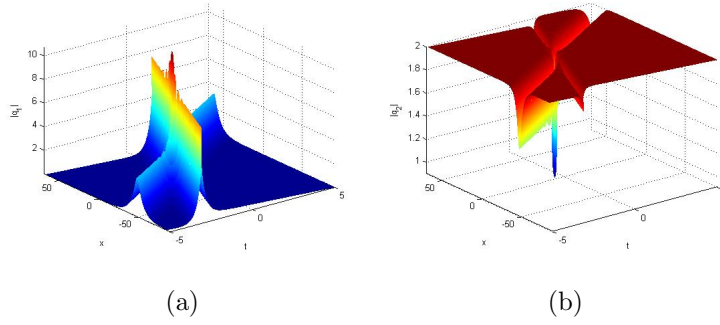


Fig. 9: Two bright-dark soliton solution to the coupled focusing-defocusing complex short pulse equation with parameters $\tau_1 = 2, k = 1, p_1 = \frac{1}{5} + \frac{1}{4}i, p_2 = \frac{3}{10} - \frac{1}{2}i, \alpha_1 = 1, \alpha_2 = \frac{1}{2}, b_1 = b_2 = 0$.

$|\tau_1(1 - \mu_{1\bar{1}})|/2$ is amplitude of the dark soliton related to the background energy. We can observe that with the background soliton parameter $|\tau_1|$ increasing, the amplitude of the bright soliton increases simultaneously (see Fig. 8), which is different from the coupled nonlinear Schrödinger equation [25].

Then the two bright-dark soliton solutions for Eqs.(4) is $q_1 = \frac{g}{f}, q_2 = \frac{h}{f}$, where

$$\begin{aligned}
f &= 1 + B_{1\bar{1}}e^{\eta_1 + \bar{\eta}_1} + B_{1\bar{2}}e^{\eta_1 + \bar{\eta}_2} + B_{2\bar{1}}e^{\eta_2 + \bar{\eta}_1} + B_{2\bar{2}}e^{\eta_2 + \bar{\eta}_2} \\
&\quad + |P_{12}|^2(P_{1\bar{1}}P_{2\bar{2}}B_{1\bar{2}}B_{2\bar{1}} - P_{1\bar{2}}P_{2\bar{1}}B_{2\bar{2}}B_{1\bar{1}})e^{\eta_1 + \eta_2 + \bar{\eta}_1 + \bar{\eta}_2}, \\
g &= a_1e^{\eta_1} + a_2e^{\eta_2} + P_{12}(a_1P_{1\bar{1}}B_{2\bar{1}} - a_2P_{2\bar{1}}B_{1\bar{1}})e^{\eta_1 + \eta_2 + \bar{\eta}_1} \\
&\quad + P_{12}(a_1P_{1\bar{2}}B_{2\bar{2}} - a_2P_{2\bar{2}}B_{1\bar{2}})e^{\eta_1 + \eta_2 + \bar{\eta}_2}, \\
h &= \tau_1e^{i(ky - \frac{\lambda}{k}s)}(1 + A_{1\bar{1}}e^{\eta_1 + \bar{\eta}_1} + A_{1\bar{2}}e^{\eta_1 + \bar{\eta}_2} + A_{2\bar{1}}e^{\eta_2 + \bar{\eta}_1} + A_{2\bar{2}}e^{\eta_2 + \bar{\eta}_2} \\
&\quad + \mu_{1\bar{1}}\mu_{2\bar{2}}|P_{12}|^2(P_{1\bar{1}}P_{2\bar{2}}B_{1\bar{2}}B_{2\bar{1}} - P_{1\bar{2}}P_{2\bar{1}}B_{2\bar{2}}B_{1\bar{1}})e^{\eta_1 + \eta_2 + \bar{\eta}_1 + \bar{\eta}_2}), \\
x &= \lambda(y + s) - 2(\ln f)_s, \quad t = -s.
\end{aligned} \tag{41}$$

where

$$\begin{aligned}
B_{j\bar{l}} &= \frac{a_j a_l^* p_j^2 p_l^{*2} (k^2 + p_j^2)(k^2 + p_l^{*2})}{4\lambda(p_j + p_l^*)^2(\lambda k^2(k^2 + p_j^2 + p_l^{*2}) + p_j^2 p_l^{*2}(\lambda - 2k^2))}, \\
A_{j\bar{l}} &= \mu_{j\bar{l}} B_{j\bar{l}}, \quad P_{ij} = \frac{p_j - p_l}{p_j + p_l}, \quad P_{j\bar{l}} = \frac{p_j - \bar{p}_l}{p_j + \bar{p}_l}, \\
\mu_{j\bar{l}} &= \frac{(k + ip_j)(k + ip_l^*)}{(k - ip_j)(k - ip_l^*)}, \quad \eta_j = p_j y + \frac{\lambda}{p_j} s + b_j \quad (j, l = 1, 2).
\end{aligned}$$

Due to $|\mu_{j\bar{l}}| = 1$, we assume $\mu_{j\bar{l}} = e^{i\phi_{jl}}$. Next we investigate the asymptotic behavior of the two bright-dark soliton solutions.

(i) Before collision ($t \rightarrow -\infty$):

Soliton 1:(the wave- η_{1R} is fixed, $\eta_{2R} \rightarrow -\infty$)

$$q_1 \rightarrow S_1^{1-} = \frac{a_1 e^{\eta_1}}{1 + e^{\eta_1^* + \eta_1 + \theta_{1\bar{1}}}} \rightarrow \frac{a_1}{2} e^{i\eta_{1R} - \frac{\theta_{1\bar{1}}}{2}} \operatorname{sech}(\eta_{1R} + \frac{\theta_{1\bar{1}}}{2}), \tag{42}$$

$$q_2 \rightarrow S_2^{1-} = \tau_1 e^{i\psi} \frac{1 + A_{1\bar{1}} e^{\eta_1 + \eta_1^*}}{1 + B_{1\bar{1}} e^{\eta_1 + \eta_1^*}} \rightarrow \frac{\tau_1}{2} e^{i\psi} [(1 + e^{\phi_{1\bar{1}}}) - (1 - e^{\phi_{1\bar{1}}}) \tanh(\eta_{1R} + \frac{\theta_{1\bar{1}}}{2})], \tag{43}$$

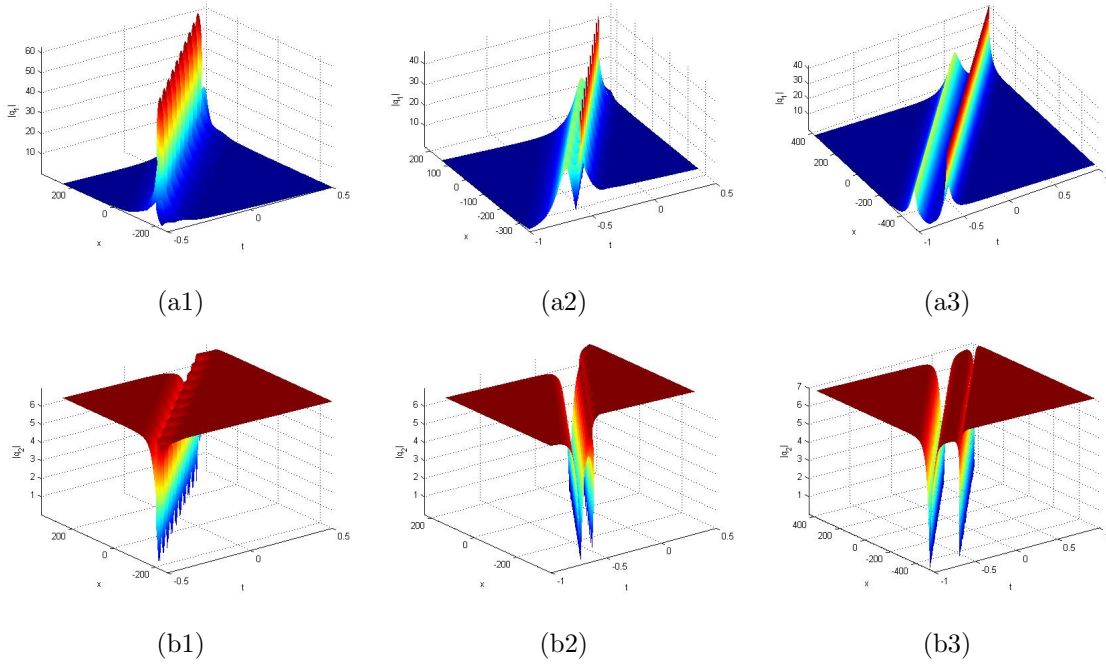


Fig. 10: Bound states of solitons for solution(41) (a1)-(b1) parameter $\tau_1 = 7$, $k = 1$, $p_1 = \frac{1}{2} + \frac{\sqrt{3}}{2}i$, $p_2 = \frac{\sqrt{3}}{2} - \frac{1}{2}i$, $a_1 = a_2 = 1$, $b_1 = 0$, $b_2 = 1$, (a2)-(b2) with the same parameters as those in (a1-b1) except for $b_1 = 1$, $b_2 = 3$, (a3)-(b3) with the same parameters as those in (a2-b2) except for $b_1 = 1$, $b_2 = 8$.

Soliton 2:(the wave- η_{2R} is fixed, $\eta_{1R} \rightarrow +\infty$)

$$q_1 \rightarrow S_1^{2-} = \frac{1}{2} e^{i\eta_{2I}} e^{\theta_{1\bar{2}1}} - (\theta_{11\bar{2}2} + \theta_{11})/2 \operatorname{sech}(\eta_{2R} + \frac{\theta_{11\bar{2}2} - \theta_{11}}{2}), \quad (44)$$

$$q_2 \rightarrow S_2^{2-} = \frac{\tau_1}{2} e^{i(\psi + \phi_{11})} [(1 + e^{\phi_{2\bar{2}}}) - (1 - e^{\phi_{2\bar{2}}}) \tanh(\eta_{2R} + \frac{\theta_{11\bar{2}2} - \theta_{11}}{2})], \quad (45)$$

where

$$G_{31} = e^{\theta_{1\bar{2}1}} = P_{12}(a_1 P_{1\bar{1}} B_{2\bar{1}} - a_2 P_{2\bar{1}} B_{1\bar{1}}),$$

$$\Omega = e^{\theta_{11\bar{2}2}} = |P_{12}|^2 (P_{1\bar{1}} P_{2\bar{2}} B_{1\bar{2}} B_{2\bar{1}} - P_{1\bar{2}} P_{2\bar{1}} B_{1\bar{1}} B_{2\bar{2}}).$$

(ii) After collision ($t \rightarrow +\infty$):

Soliton 1:(the wave- η_{1R} is fixed, $\eta_{2R} \rightarrow +\infty$)

$$q_1 \rightarrow S_1^{1+} = \frac{1}{2} e^{i\eta_{1I}} e^{\theta_{122}} - (\theta_{11\bar{2}2} + \theta_{2\bar{2}})/2 \operatorname{sech}(\eta_{1R} + \frac{\theta_{11\bar{2}2} - \theta_{2\bar{2}}}{2}), \quad (46)$$

$$q_2 \rightarrow S_2^{1+} = \frac{\tau_1}{2} e^{i(\psi + \phi_{2\bar{2}})} [(1 + e^{\phi_{1\bar{1}}}) - (1 - e^{\phi_{1\bar{1}}}) \tanh(\eta_{1R} + \frac{\theta_{11\bar{2}2} - \theta_{2\bar{2}}}{2})], \quad (47)$$

where

$$G_{32} = e^{\theta_{122}} = P_{12}(\alpha_1 P_{1\bar{2}} B_{2\bar{2}} - \alpha_2 P_{2\bar{2}} B_{1\bar{2}}).$$

Soliton 2:(the wave- η_{2R} is fixed, $\eta_{1R} \rightarrow -\infty$)

$$q_1 \rightarrow S_1^{2+} = \frac{a_2 e^{\eta_2}}{1 + e^{\eta_2 + \eta_2 + \theta_{2\bar{2}}}} \rightarrow \frac{a_2}{2} e^{i\eta_{2I} - \frac{\theta_{2\bar{2}}}{2}} \operatorname{sech}(\eta_{2R} + \frac{\theta_{2\bar{2}}}{2}), \quad (48)$$

$$q_2 \rightarrow S_2^{2+} = \tau_1 e^{i\psi} \frac{1 + A_{2\bar{2}} e^{\eta_2 + \eta_2^*}}{1 + B_{2\bar{2}} e^{\eta_2 + \eta_2^*}} \rightarrow \frac{\tau_1}{2} e^{i\psi} [(1 + e^{\phi_{2\bar{2}}}) - (1 - e^{\phi_{2\bar{2}}}) \tanh(\eta_{2R} + \frac{\theta_{2\bar{2}}}{2})]. \quad (49)$$

with

$$B_{i\bar{j}} = e^{\theta_{i\bar{j}}} \quad (i = 1, 2)$$

Table 2: Physical quantities of bright-dark soliton S_1 and S_2 before and after interactions.

Soliton	Amplitude/depth	Velocity	Soliton	Amplitude/depth	Velocity
S_1^{1-}	$\sqrt{\frac{a_1 a_1^*}{4B_{1\bar{1}}}}$	$-\frac{ \tau_1 ^2}{2 p_1 ^2}$	S_1^{1+}	$\sqrt{\frac{G_{32} G_{32}^*}{4\Omega B_{2\bar{2}}}}$	$-\frac{ \tau_1 ^2}{2 p_1 ^2}$
S_2^{1-}	$ \tau_1 \sqrt{\frac{1 + \mu_{1\bar{1}}}{2} \frac{\mu_{1\bar{1}} - 1}{2}}$	$-\frac{ \tau_1 ^2}{2 p_1 ^2}$	S_2^{1+}	$ \tau_1 \sqrt{\frac{1 + \mu_{1\bar{1}}}{2} \frac{\mu_{1\bar{1}} - 1}{2}}$	$-\frac{ \tau_1 ^2}{2 p_1 ^2}$
S_1^{2-}	$\sqrt{\frac{G_{32} G_{32}^*}{4\Omega B_{1\bar{1}}}}$	$-\frac{ \tau_1 ^2}{2 p_2 ^2}$	S_1^{2+}	$\sqrt{\frac{a_2 a_2^*}{4B_{2\bar{2}}}}$	$-\frac{ \tau_1 ^2}{2 p_2 ^2}$
S_2^{2-}	$ \tau_1 \sqrt{\frac{1 + \mu_{2\bar{2}}}{2} \frac{\mu_{2\bar{2}} - 1}{2}}$	$-\frac{ \tau_1 ^2}{2 p_2 ^2}$	S_2^{2+}	$ \tau_1 \sqrt{\frac{1 + \mu_{2\bar{2}}}{2} \frac{\mu_{2\bar{2}} - 1}{2}}$	$-\frac{ \tau_1 ^2}{2 p_2 ^2}$

Through the direct calculation, we get

$$\frac{|a_1|}{\sqrt{B_{1\bar{1}}}} = \frac{|G_{32}|}{\sqrt{\Omega B_{2\bar{2}}}}, \quad \frac{|a_2|}{\sqrt{B_{2\bar{2}}}} = \frac{|G_{31}|}{\sqrt{\Omega B_{1\bar{1}}}}.$$

From Table 2, we can see that the velocities and amplitude of both bright and dark solitons keep unchanged before and after collisions except a phase shift.

Remark 2: For the one soliton solution, the parameter p_1 denotes the direction of the soliton and τ_1 , a_1 give its amplitude. The one-soliton solution is characterized by five parameters τ_1 , a_1 , b_1 , k , λ . τ_1 is restricted by the parameters k , p_1 . Now the role of parameter a_1 can be realized explicitly in the amplitude (intensity) of bright component. This is shown in Fig.(7). The dark soliton part influences the bright part through the parameters τ_1 (see Fig.(8)). For the two bright-dark soliton, when $|p_1| = |p_2|$, the two solitons travel in parallel. Due to the velocities of solitons and distance between the solitons, oblique interactions, attraction, exclusion soliton periodically will happen [28]. Fig. 9 and Fig. 10 show different kinds of soliton collisions.

3.2 Dark-dark soliton solution

In order to get dark-dark soliton solutions, we assume $g_j = g_0^{(j)}(1 + \chi g_1^{(j)} + \chi^2 g_2^{(j)} + \dots)$ ($j = 1, 2$) and $f = 1 + \chi f_1 + \chi^2 f_2 + \dots$ where $g_k^{(j)}$ ($k = 1, 2, \dots$) are complex functions and f_k are real functions. Substituting these forms into (35) and collecting the coefficients of χ_0 , yields $g_0^{(j)} = \tau_j e^{i\psi_j}$, $\psi_j = k_j y - \frac{\lambda}{k_j} s + \psi_j^{(0)}$ with $\lambda = \frac{1}{2}(|\tau_2|^2 - |\tau_1|^2)$, in which $k_j, \psi_j^{(0)}$ are real constants and τ_j are complex constants.

Eliminating $g_0^{(j)}$, we still use g_j substituting g_j for convenience. Then the bilinear equation(35) can be rewritten as

$$\begin{aligned} (D_s D_y - ik_j D_s + \frac{i\lambda}{k_j} D_y) f \cdot g_j &= 0, \\ (D_s^2 - \lambda) f \cdot f &= \frac{1}{2} (|\tau_1 g_1|^2 - |\tau_2 g_2|^2), \end{aligned} \quad (50)$$

where $g_j = 1 + \chi g_1^{(j)} + \chi^2 g_2^{(j)} + \dots$. Then the equation (50) admits the solutions

$$g_1^{(j)} = Z_1^{(j)} e^{\eta_1}, \quad f_1 = e^{\eta_1}, \quad \eta_1 = P_1 y - \Omega_1 s + \eta_1^{(0)}, \quad (51)$$

in which P_1 , Ω_1 , and $\eta_1^{(0)}$ are real constants and $Z_1^{(j)}$ are complex constants. Collecting the coefficients of χ_1 from (50), we have

$$Z_1^{(j)} = \frac{-P_1 \Omega_1 + i(k_j \Omega_1 + \frac{\lambda}{k_j} P_1)}{P_1 \Omega_1 + i(k_j \Omega_1 + \frac{\lambda}{k_j} P_1)} \quad (j = 1, 2), \quad (52)$$

where

$$\frac{|\tau_2|^2}{(P_1 \Omega_1)^2 + (k_2 \Omega_1 + \frac{\lambda}{k_2} P_1)^2} - \frac{|\tau_1|^2}{(P_1 \Omega_1)^2 + (k_1 \Omega_1 + \frac{\lambda}{k_1} P_1)^2} = \frac{1}{P_1^2}. \quad (53)$$

It's obvious that $|Z_1^{(j)}| = 1$ and $g_k^{(j)} = f_k = 0$, ($j = 1, 2, k = 2, 3, \dots$). Thus the one dark soliton solution is written as

$$q_j = \frac{1}{2} \tau_j e^{i\psi_j} [(1 + Z_1^{(j)}) - (1 - Z_1^{(j)}) \tanh(\frac{\eta_1}{2})], \quad (54)$$

$$x = \lambda(y + s) + \frac{2\Omega_1 e^{\eta_1}}{1 + e^{\eta_1}}, \quad t = -s. \quad (55)$$

To analyze the dynamics of the one-soliton solution for the Eq.(7), we should know the term $\partial x / \partial y$. Although it is difficult to classify the types of soliton like the bright soliton because the parameters P_1 and Ω_1 can not be determined independently, we can solve Ω_1, P_1 in the special case $k_j = k$ ($j = 1, 2$). Letting $Z_1^{(j)} = e^{2i\theta_1}$, it follows that

$$\Omega_1 = \sqrt{2\lambda} \sin \theta_1, \quad P_1 = \frac{2k^2 \sin \theta_1}{2k \cos \theta_1 - \sqrt{2\lambda}}. \quad (56)$$

Since

$$\frac{\partial x}{\partial y} = \frac{\lambda + (2\lambda + \frac{4\sqrt{2\lambda}k^2 \sin^2 \theta_1}{2k \cos \theta_1 - \sqrt{2\lambda}})e^{\eta_1} + \lambda e^{2\eta_1}}{(1 + e^{\eta_1})^2}, \quad (57)$$

we classify this one-dark soliton solution as follows:

- (i) when $\sqrt{2\lambda} - 2k \cos \theta_1 < 0$, or $\sqrt{2\lambda} - 2k \cos \theta_1 > 0$ and $\Delta_1 > 0$, where $\Delta_1 = \lambda - \sqrt{2\lambda}k \cos \theta_1 - 2k^2 \sin^2 \theta_1$ the single-dark soliton solution is always smooth. An example is illustrated in Fig. 11(b1).
- (ii) when $\sqrt{2\lambda} - 2k \cos \theta_1 > 0$ and $\Delta_1 = 0$, then the $\partial x / \partial y$ attains zero at only one point, which leads to a cusped dark soliton as displayed in Fig. 11(b2).
- (iii) when $\sqrt{2\lambda} - 2k \cos \theta_1 > 0$ and $\Delta_1 < 0$, then the $\partial x / \partial y$ attains zero at two point, which leads to a loop dark soliton as displayed in Fig. 11(b3).

To construct the two dark-dark soliton solution, we assume

$$\begin{aligned} g_1^{(j)} &= \gamma_1^{(j)} e^{\eta_1} + \gamma_2^{(j)} e^{\eta_2}, \quad f_1 = e^{\eta_1} + e^{\eta_2}, \\ g_2^{(j)} &= \gamma_1^{(j)} \gamma_2^{(j)} \nu e^{\eta_1 + \eta_2}, \quad f_2 = \nu e^{\eta_1 + \eta_2}, \\ \eta_j &= P_j y - \Omega_j s + \eta_j^{(0)}, \quad (j = 1, 2). \end{aligned} \quad (58)$$

Substituting (58) into (50) and collecting the terms with the same power of χ , we have

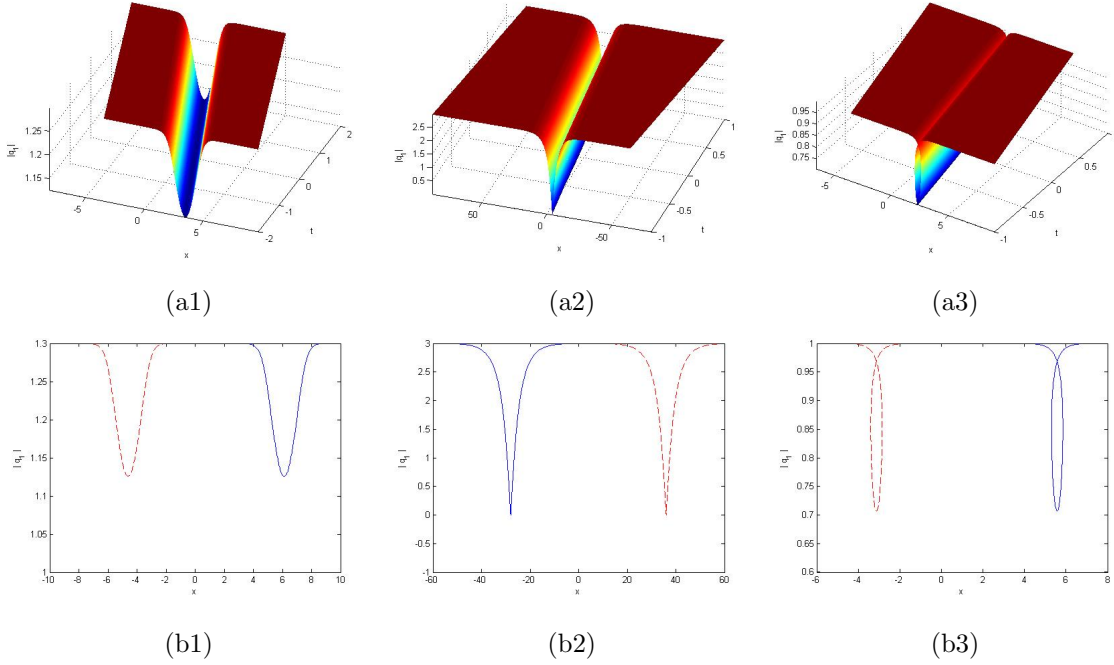


Fig. 11: One dark soliton to the coupled focusing-defocusing complex short pulse equation: (a) 3D plot. (b) profiles of $|q|$ at $t = -4$ (blue solid line); $t = 4$ (magenta dashed line). (a1)-(b1) smooth soliton with $\tau_1 = 1.3$, $\tau_2 = 2$, $k = 1, \theta_1 = \frac{\pi}{6}, \eta_1^{(0)} = 0$, (a2)-(b2) cuspon soliton with $\tau_1 = 3$, $\tau_2 = 5$, $k = 2, \theta_1 = \frac{\pi}{2}, \eta_1^{(0)} = 0$, (a3)-(b3) loop soliton with $\tau_1 = 1$, $\tau_2 = 2$, $k = 1, \theta_1 = \frac{\pi}{4}, \eta_1^{(0)} = 0$.

$$\gamma_l^{(j)} = \frac{-P_l \Omega_l + i(k_j \Omega_l + \frac{\lambda}{k_j} P_l)}{P_l \Omega_l + i(k_j \Omega_l + \frac{\lambda}{k_j} P_l)}, \quad (j, l = 1, 2) \quad (59)$$

$$\nu = \frac{P_1 P_2 \Omega_1 \Omega_2 (P_1 - P_2) (\Omega_2 - \Omega_1) + \lambda (P_2 \Omega_1 - P_1 \Omega_2)^2}{-P_1 P_2 \Omega_1 \Omega_2 (P_1 + P_2) (\Omega_1 + \Omega_2) + \lambda (P_2 \Omega_1 - P_1 \Omega_2)^2}, \quad (60)$$

where P_j and Ω_j satisfy

$$\frac{|\tau_2|^2}{(P_j \Omega_j)^2 + (k_2 \Omega_j + \frac{\lambda}{k_2} P_j)^2} - \frac{|\tau_1|^2}{(P_j \Omega_j)^2 + (k_1 \Omega_j + \frac{\lambda}{k_1} P_j)^2} = \frac{1}{P_j^2} \quad (j = 1, 2). \quad (61)$$

Then we get the dark-dark soliton solutions for Eq.(7)

$$q_j = \tau_j e^{i(k_j y - \frac{\lambda}{k_j} s)} \frac{1 + \gamma_1^{(j)} e^{\eta_1} + \gamma_2^{(j)} e^{\eta_2} + \gamma_1^{(j)} \gamma_2^{(j)} \nu e^{\eta_1 + \eta_2}}{1 + e^{\eta_1} + e^{\eta_2} + \nu e^{\eta_1 + \eta_2}}, \quad (j = 1, 2) \quad (62)$$

$$x = \lambda(y + s) + 2 \frac{\Omega_1 e^{\eta_1} + \Omega_2 e^{\eta_2} + (\Omega_1 + \Omega_2) \nu e^{\eta_1 + \eta_2}}{1 + e^{\eta_1} + e^{\eta_2} + \nu e^{\eta_1 + \eta_2}}, \quad t = -s. \quad (63)$$

To show that the solution indeed gives a dark-dark soliton for Eq.(7), we consider its asymptotic behavior. We assume $P_{1R}, P_{2R}, \Omega_{1R}, \Omega_{2R} > 0$, $\frac{P_{1R}}{P_{2R}} > \frac{\Omega_{1R}}{\Omega_{2R}}$ without loss of generality. Then we discuss the following two cases:

(i) when the wave- η_{1R} is fixed, $\eta_{2R} = \frac{P_{2R}}{P_{1R}} \eta_{1R} - (\Omega_{2R} - \frac{P_{2R}}{P_{1R}} \Omega_{1R})s$. When $t \rightarrow \pm\infty$, we have $\eta_{2R} \rightarrow \pm\infty$ for soliton

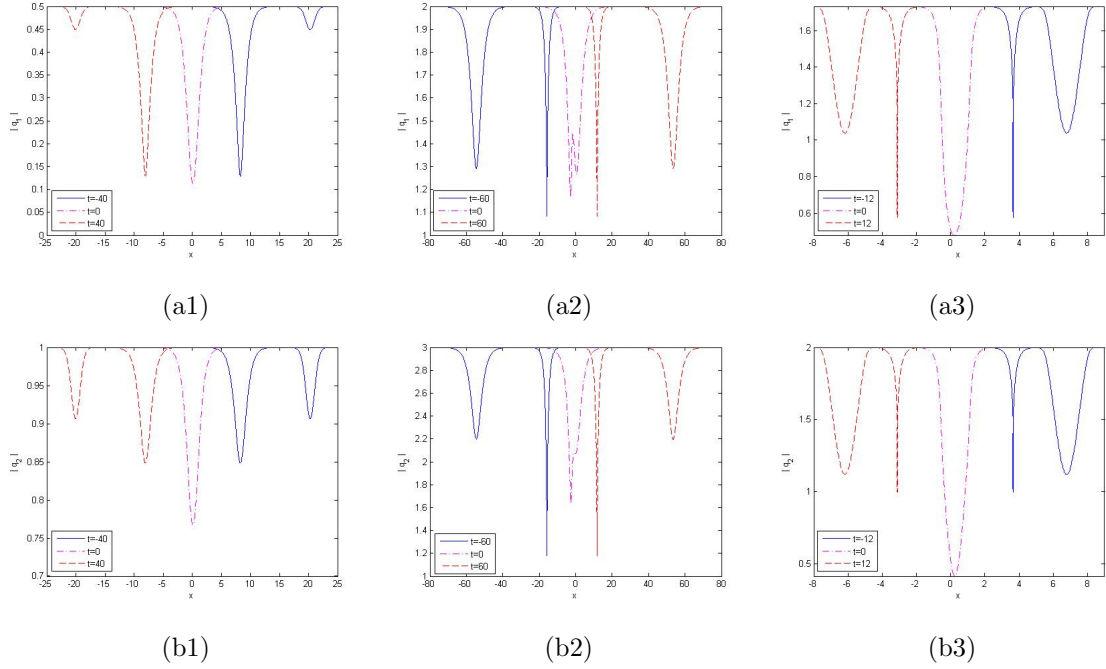


Fig. 12: Evolution plot of two dark-dark soliton solution for(58) with parameters $\eta_1^{(0)} = \eta_2^{(0)} = 0$. (a1)-(b1) parameters $\tau_1 = \frac{1}{2}$, $\tau_2 = 1$, $k_1 = 1, k_2 = \sqrt{2}, P_1 = 1, P_2 = \frac{1}{2}, \Omega_1 \approx 0.35960053, \Omega_2 \approx -0.21633656$, (a2)-(b2) parameters $\tau_1 = \sqrt{3} - i$, $\tau_2 = \sqrt{5} + 2i$, $k_1 = 1, k_2 = 2, P_1 = 2, P_2 = 1, \Omega_1 \approx -2.18581909, \Omega_2 \approx -1.35443428$, (a3)-(b3) parameters $\tau_1 = 1 + \sqrt{2}i$, $\tau_2 = 1 - \sqrt{3}i$, $k_1 = 1, k_2 = 1, P_1 = 2, P_2 = 5, \Omega_1 \approx -0.58595167, \Omega_2 \approx 0.90979099$.

1. (ii) When the wave- η_{2R} is fixed, $\eta_{1R} = \frac{P_{1R}}{P_{2R}}\eta_{2R} - (\Omega_{1R} - \frac{P_{1R}}{P_{2R}}\Omega_{2R})s$. When $t \rightarrow \pm\infty$, $\eta_{1R} \rightarrow \mp\infty$ for soliton 2. This leads to the following asymptotic forms for two-soliton solution under the reciprocal transformation(63).

(i)Soliton 1:(the wave- η_{1R} is fixed, $\eta_{2R} \rightarrow \mp\infty$),

$$q_j \sim \begin{cases} \frac{1}{2}\tau_j e^{i\psi_j} [(1 + \gamma_1^{(j)}) - (1 - \gamma_1^{(j)}) \tanh(\frac{\eta_1}{2})] & (t \rightarrow -\infty), \\ \frac{1}{2}\tau_j \gamma_2^{(j)} e^{i\psi_j} [(1 + \gamma_1^{(j)}) - (1 - \gamma_1^{(j)}) \tanh(\frac{\eta_1}{2} + \eta_{10})] & (t \rightarrow +\infty), \end{cases} \quad (64)$$

(ii)Soliton 2:(the wave- η_{2R} is fixed,, $\eta_{1R} \rightarrow \pm\infty$),

$$q_j \sim \begin{cases} \frac{1}{2}\tau_j \gamma_1^{(j)} e^{i\psi_j} [(1 + \gamma_2^{(j)}) - (1 - \gamma_2^{(j)}) \tanh(\frac{\eta_2}{2} + \eta_{10})] & (t \rightarrow -\infty), \\ \frac{1}{2}\tau_j e^{i\psi_j} [(1 + \gamma_2^{(j)}) - (1 - \gamma_2^{(j)}) \tanh(\frac{\eta_2}{2})] & (t \rightarrow +\infty). \end{cases} \quad (65)$$

Remark 3: From the analysis of the asymptotic behavior of the two dark-dark solitons, we can see that the interaction of the two solitons are elastic. The collision processes between smooth-smooth dark solitons, smooth-cuspon dark solitons and smooth-loop dark solitons are illustrated in Fig.11(a1-a3), respectively. When a smooth dark soliton interacts with a cuspon dark soliton, the singularity of the cuspon dark soliton maintains as observed in Fig.12(a2-b2) and Fig.12(a3-b3), which is different from the interaction of the dark soliton of defocusing CSP equation [22].

Especially, when $k_j = k(j = 1, 2, \dots, N)$, the explicit N-dark soliton solutions for Eq.(7) can be written as

$$\begin{aligned} q_{1,N} &= \tau_1 e^{i(ky - \frac{\lambda}{k}s)} \frac{\sum_{\mu=0,1} e^{\sum_{j=1}^n \mu_j (\eta_j + 2i\theta_j)} + \sum_{1 \leq j < l}^n \mu_j \mu_l A_{jl}}{\sum_{\mu=0,1} e^{\sum_{j=1}^n \mu_j \eta_j} + \sum_{1 \leq j < l}^n \mu_j \mu_l A_{jl}}, \\ q_{2,N} &= \tau_2 e^{i(ky - \frac{\lambda}{k}s)} \frac{\sum_{\mu=0,1} e^{\sum_{j=1}^n \mu_j (\eta_j + 2i\theta_j)} + \sum_{1 \leq j < l}^n \mu_j \mu_l A_{jl}}{\sum_{\mu=0,1} e^{\sum_{j=1}^n \mu_j \eta_j} + \sum_{1 \leq j < l}^n \mu_j \mu_l A_{jl}}, \end{aligned} \quad (66)$$

where

$$\begin{aligned} \eta_j &= P_j y - \Omega_j s + \eta_j^{(0)}, e^{A_{jl}} = \left(\frac{\sin \frac{\theta_j - \theta_l}{l}}{\sin \frac{\theta_j + \theta_l}{l}} \right)^2, \\ \Omega_j &= \sqrt{|\tau_2|^2 - |\tau_1|^2} \sin \theta_j, \quad P_j = \frac{2k^2 \sin \theta_j}{2k \cos \theta_j - \sqrt{|\tau_2|^2 - |\tau_1|^2}}, \\ x &= \lambda(y + s) - 2[\ln(\sum_{\mu=0,1} e^{\sum_{j=1}^n \mu_j \eta_j} + \sum_{1 \leq j < l}^n \mu_j \mu_l A_{jl})]_s, \quad t = -s. \end{aligned} \quad (67)$$

4 Breather and rogue wave solutions

4.1 Breather solution

We know the breather soliton solution can be derived from dark-dark soliton solution. In this section, we will give the breather soliton to Eq.(7) from Eq.(62). We assume $\Omega_j, \eta_j^{(0)}$ are complex and k_j ($j = 1, 2$) are still real constants, and set $\eta_2 = \eta_1^* = \eta$ and $\phi_2 = \phi_1^* \pm \pi$, $\varphi_2 = \varphi_1^* \pm \pi$. $\phi_1 = \phi_R + i\phi_I$, $\varphi_1 = \varphi_R + i\varphi_I$. Then q_1, q_2 can be rewritten as

$$\begin{aligned} q_1 &= \tau_1 e^{i(\psi_1 + 2\phi_R)} \frac{\sqrt{\nu} \cosh(\eta_R + 2i\phi_R + \sigma) + \cos(\eta_I + 2i\phi_I)}{\sqrt{\nu} \cosh(\eta_R + \sigma) + \cos \eta_I}, \\ q_2 &= \tau_2 e^{i(\psi_2 + 2\varphi_R)} \frac{\sqrt{\nu} \cosh(\eta_R + 2i\varphi_R + \sigma) + \cos(\eta_I + 2i\varphi_I)}{\sqrt{\nu} \cosh(\eta_R + \sigma) + \cos \eta_I}, \\ x &= \lambda(y + s) + \frac{2\sqrt{\nu} \sinh(\eta_R + \sigma) - \Omega_I \sin \eta_I}{\sqrt{\nu} \cosh(\eta_R + \sigma) + \cos \eta_I}, \quad t = -s. \end{aligned} \quad (68)$$

where $\eta = \eta_R + i\eta_I$, $P_1 = P_R + iP_I$, $\Omega_1 = \Omega_R + i\Omega_I$, $\eta_R = P_R y - \Omega_R s + \eta_R^{(0)}$, $\eta_I = P_I y - \Omega_I s + \eta_I^{(0)}$, $\sigma = \frac{1}{2} \ln \nu$, $\phi_R = \ln |\gamma_1^{(1)}|$, $\phi_I = \arg(\gamma_1^{(1)})$, $\varphi_R = \ln |\gamma_1^{(2)}|$, $\varphi_I = \arg(\gamma_1^{(2)})$, where P_1, Ω_1 and ν satisfy

$$\begin{aligned} \lambda &= \frac{|\tau_2|^2 - |\tau_1|^2}{2}, \quad \gamma_1^{(j)} = \frac{-P_1 \Omega_1 + i(k_j \Omega_1 + \frac{\lambda}{k_j} P_1)}{P_1 \Omega_1 + i(k_j \Omega_1 + \frac{\lambda}{k_j} P_1)}, \quad (j = 1, 2), \\ \nu &= \frac{-P_I \Omega_I |P_1 \Omega_1|^2 + \lambda(P_R \Omega_I - P_I \Omega_R)^2}{P_R \Omega_R |P_1 \Omega_1|^2 + \lambda(P_R \Omega_I - P_I \Omega_R)^2}, \end{aligned} \quad (69)$$

$$\frac{1}{P_1^2} = \frac{|\tau_2|^2}{(P_1 \Omega_1)^2 + (k_2 \Omega_1 + \frac{\lambda}{k_2} P_1)^2} - \frac{|\tau_1|^2}{(P_1 \Omega_1)^2 + (k_1 \Omega_1 + \frac{\lambda}{k_1} P_1)^2}. \quad (70)$$

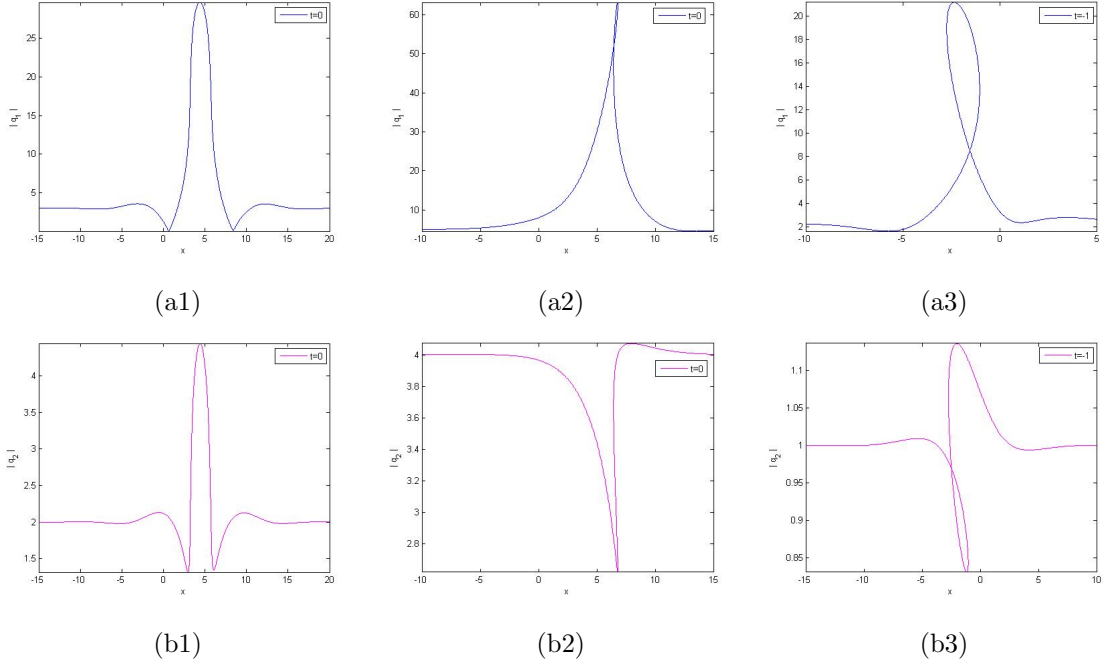


Fig. 13: Evolution breathers for Eq.(7). (a1)-(b1)Smooth breather with parameters $\tau_1 = 3, \tau_2 = 2, k_1 = 1, k_2 = 2, P_1 = 1 + \sqrt{3}i, \Omega_1 \approx 1.54849728 - 5.02607499i, \eta^{(0)} = 0$, (a2)-(b2)Breather with parameters $\tau_1 = 5, \tau_2 = 4, k_1 = \frac{1}{2}, k_2 = \frac{1}{4}, P_1 = 2 - i, \Omega_1 \approx 1.43479848 - 9.30893675i, \eta^{(0)} = 0$, (a3)-(b3)loop breather with parameters $\tau_1 = 1 + 2i, \tau_2 = 1, k_1 = \frac{1}{2}, k_2 = \frac{1}{4}, P_1 = 1 + i, \Omega_1 \approx 1.60552879 - 5.39497000i, \eta^{(0)} = 0$.

Especially, when $k_j = k(j = 1, 2)$, we rewrite q_1, q_2 as

$$q_1 = \tau_1 e^{i(\psi + 2\theta_R)} \frac{\sqrt{\nu} \cosh(\eta_R + 2i\theta_R + \sigma) + \cos(\eta_I + 2i\theta_I)}{\sqrt{\nu} \cosh(\eta_R + \sigma) + \cos \eta_I},$$

$$q_2 = \tau_2 e^{i(\psi + 2\theta_R)} \frac{\sqrt{\nu} \cosh(\eta_R + 2i\theta_R + \sigma) + \cos(\eta_I + 2i\theta_I)}{\sqrt{\nu} \cosh(\eta_R + \sigma) + \cos \eta_I}, \quad (71)$$

$$x = \lambda(y + s) + \frac{2\sqrt{\nu} \sinh(\eta_R + \sigma) - \Omega_I \sin \eta_I}{\sqrt{\nu} \cosh(\eta_R + \sigma) + \cos \eta_I}, \quad t = -s, \quad (72)$$

where

$$\Delta = \sqrt{|\tau_1|^2 - |\tau_2|^2}, \quad \nu = \frac{\cosh^2 \theta_I}{\cos^2 \theta_R},$$

$$\Omega_R = -\Delta \cos \theta_R \sinh \theta_I, \quad \Omega_I = \Delta \sin \theta_R \cosh \theta_I,$$

$$P_R = \frac{2k^2 \cos \theta_R (2k \sin \theta_R - \Delta \sinh \theta_I)}{(\Delta + 2k \sin \theta_R \sinh \theta_I)^2 + (2k \cos \theta_R \cosh \theta_I)^2}, \quad (73)$$

$$P_I = \frac{2k^2 \cosh \theta_I (\Delta \sin \theta_R + 2k \sinh \theta_I)}{(\Delta + 2k \sin \theta_R \sinh \theta_I)^2 + (2k \cos \theta_R \cosh \theta_I)^2}.$$

Remark 4: Fig.13 illustrates the 2D plots of the breather soliton solution(68) at time $t = 0$. From the Figs.14(a) and 14(b), we observe that due to the hodograph transformation(72), when $\theta_{1R} = 0$ or $\theta_{1I} = 0$, the Akhmediev

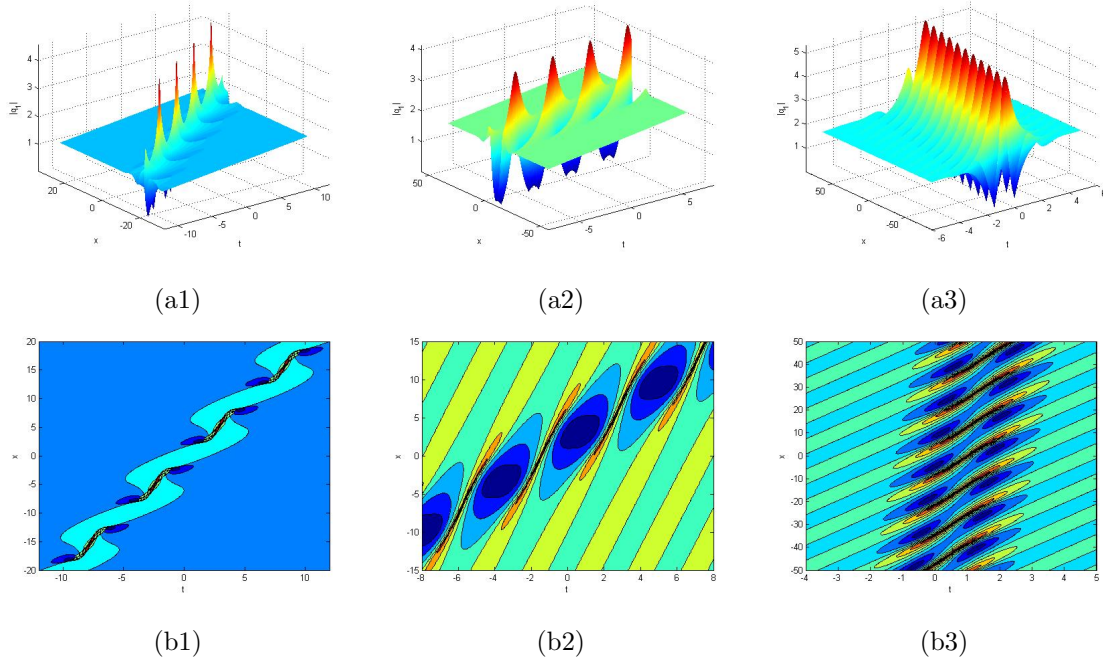


Fig. 14: 3D and contour plots of the breather soliton for the Eq.(7) with parameter $k = 1, \eta^{(0)} = 0$. (a1) parameter with $\tau_1 = 1.4, \tau_2 = 1, \theta_R = 0, \theta_I = \frac{1}{2}$, (a2) parameter with $\tau_1 = 2, \tau_2 = 1, \theta_R = 1, \theta_I = 0$, (a3) parameter with $\tau_1 = 2, \tau_2 = 1, \theta_R = 1, \theta_I = 1$

breather and Ma breather are no longer existence which is different from the GCNLS [33].

4.2 Rogue wave soliton solutions

The rogue wave appeared in the nonlinear system has been widely studied [35–40]. In order to construct the rogue wave solution to coupled focusing-defocusing complex short pulse equation(7), we consider the breather solution (68). Let $P_1 = \varepsilon$ and ε is a complex small parameter. From the expression(70), we have $\Omega_1 = \omega_1\varepsilon + o(\varepsilon)$, where ω_1 satisfies

$$|k_2\tau_2|^2(\lambda + \omega_1 k_1^2)^2 - (\lambda + \omega_1 k_2^2)^2(|k_1\tau_1|^2 + (\lambda + \omega_1 k_1^2)^2) = 0 \quad (74)$$

If $\eta_1^{(0)} = i\pi$, then $\eta_1 = \varepsilon(x - \omega_1 t) + i\pi + o(\varepsilon^2)$, and

$$\begin{aligned} \gamma_1^{(j)} &= 1 + \frac{2ik_j\omega_1\varepsilon}{\lambda + k_j^2\omega_1} - \frac{2(k_j\omega_1)^2\varepsilon^2}{(\lambda + k_j^2\omega_1)^2} + O(\varepsilon^2), \\ \gamma_2^{(j)} &= 1 + \frac{2ik_j\omega_1^*\varepsilon^*}{\lambda + k_j^2\omega_1^*} - \frac{2(k_j\omega_1^*)^2\varepsilon^{*2}}{(\lambda + k_j^2\omega_1^*)^2} + O(\varepsilon^{*2}), \\ \nu &= 1 + \frac{2(\omega_1 + \omega_1^*)|\omega_1|^2|\varepsilon|^2}{\lambda(\omega_1 - \omega_1^*)^2} + O(\varepsilon^2, \varepsilon^{*2}, |\varepsilon|^2). \end{aligned}$$

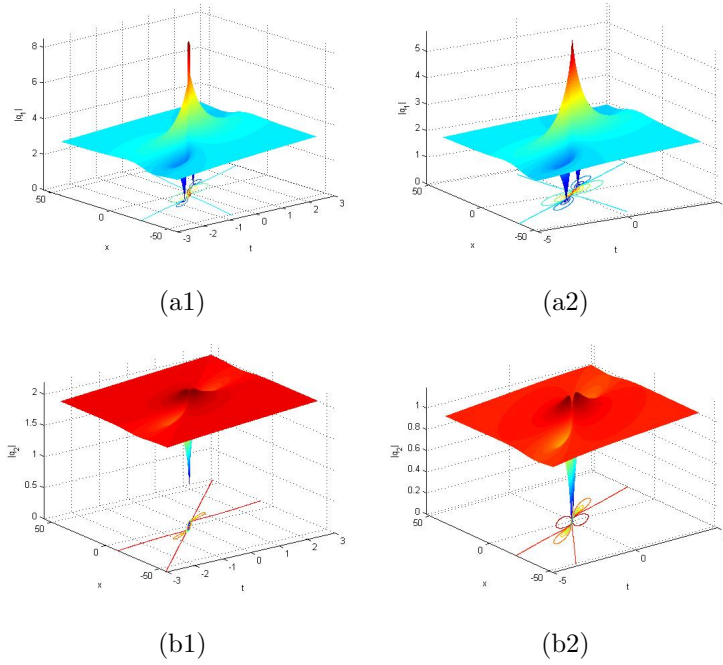


Fig. 15: Rogue wave for Eq.(7) with the contour line drawn at the bottom of the figure. (a1)-(b1) q_1 is a bright rogue wave. q_2 is a dark rogue wave with parameter $\tau_1 = 3, \tau_2 = 2, k_1 = 1, k_2 = 2, \omega_1 \approx 2.60485 + 2.95036i$. (a2)-(b2) q_1 and q_2 are four-petals rogue wave with parameter $\tau_1 = 2, \tau_2 = 1, k_1 = \frac{2}{3}, k_2 = 1, \omega_1 \approx 3.479849 - 2.95036i$.

We thus have,

$$\begin{aligned}
f &= (|y - \omega_1 s|^2 + \frac{2(\omega_1 + \omega_1^*)|\omega_1|^2}{\lambda(\omega_1 - \omega_1^*)^2})|\varepsilon|^2 + O(\varepsilon^2, \varepsilon^{*2}, |\varepsilon|^2), \\
g_j &= (|y - \omega_1 s|^2 + \frac{2(\omega_1 + \omega_1^*)|\omega_1|^2}{\lambda(\omega_1 - \omega_1^*)^2} + \frac{2ik_j\omega_1(y - \omega_1^*s)}{\lambda + k_j^2\omega_1} + \frac{2ik_j\omega_1^*(y - \omega_1 s)}{\lambda + k_j^2\omega_1^*} \\
&\quad - \frac{4k_j^2|\omega_1|^2}{|\lambda + k_j^2\omega_1|^2}) + O(\varepsilon^2, \varepsilon^{*2}, |\varepsilon|^2), \quad (j = 1, 2).
\end{aligned} \tag{75}$$

Taking the limit $\varepsilon \rightarrow 0$, and letting $\omega_1 = \mu + iv$, the rogue wave is written as

$$q_j = \tau_j e^{i\psi_j} \left(1 + 4\frac{L}{M}\right), \tag{76}$$

where

$$\begin{aligned}
L &= \lambda(k_j v)^2(\mu^2 + v^2) - i\lambda k_j v^2((\lambda\mu + k_j^2(\mu^2 + v^2))(y - \mu s) + \lambda v^2 s), \\
M &= (\lambda^2 + 2\lambda\mu k_j^2 + k_j^4(\mu^2 + v^2))(\mu^3 + v^2(\mu - \lambda(y - s\mu)^2) - \lambda v^4 s^2), \\
x &= \lambda(y + s) - \frac{4v^2((\mu^2 + v^2)s - \mu y)}{v^2(\lambda(y - \mu s)^2 - \mu) + \lambda v^4 s^2}, \quad t = -s(j = 1, 2).
\end{aligned}$$

the real number μ, v can still be determined by ω_1 from(74).

$$\begin{aligned} & \lambda^4 + (\lambda k_2)^2(2\lambda\mu + (\mu^2 - v^2)k_2^2 - |\tau_2|^2) + k_1^2(\lambda^2(2\lambda\mu + |\tau_1|^2) + k_2^4(2\lambda\mu(\mu^2 - 3v^2) + (\mu^2 - v^2)|\tau_1|^2) \\ & + 2\lambda k_2^2(2\lambda(\mu^2 - v^2) + \mu(|\tau_1|^2 - |\tau_2|^2))) + k_1^4(\lambda^2(\mu^2 - v^2) + k_2^4(\mu^4 - 6\mu^2v^2 + v^4) \\ & + k_2^2(2\lambda\mu(\mu^2 - 3v^2) + (v^2 - \mu^2)|\tau_2|^2)) = 0, \\ & 2v(\lambda^2 k_2^2(\lambda + \mu k_2^2) + k_1^2(\lambda^3 + k_2^4(3\lambda\mu^2 - \lambda v^2 + \mu|\tau_1|^2) + \lambda k_2^2(4\lambda\mu + |\tau_1|^2 - |\tau_2|^2)) \\ & + k_1^4(\lambda^2\mu + 2\mu k_2^4(\mu^2 - v^2) + k_2^2(3\lambda\mu^2 - \lambda v^2 - \mu|\tau_2|^2))) = 0. \end{aligned}$$

The analytical expression of the rogue wave is given with six parameters. Through the direct calculation, we can find that there exist four extreme points. The amplitude of the central point is

$$|q_j(0, 0)|^2 = |\tau_j|^2 \frac{(\lambda^2\mu + 2\lambda k_j^2(\mu^2 + 2v^2) + \mu k_j^4(\mu^2 + v^2))^2}{\mu^2(\lambda^2 + 2\lambda\mu k_j^2 + k_j^4(\mu^2 + v^2))^2}, \quad (j = 1, 2).$$

We ignore the analysis of the other extreme points as the formulas are tedious and complicated. The bright rogue wave and dark rogue wave are described in Fig.15(a1)and Fig.15(b1) respectively and the four-petal rogue wave is also received in Fig.15(a2)-(b2). It should be remark here that the dark rogue wave has not been reported in the short pulse equation.

To analyze the dynamics of the rogue wave solution for the Eq.(7), we need to solve the relation between

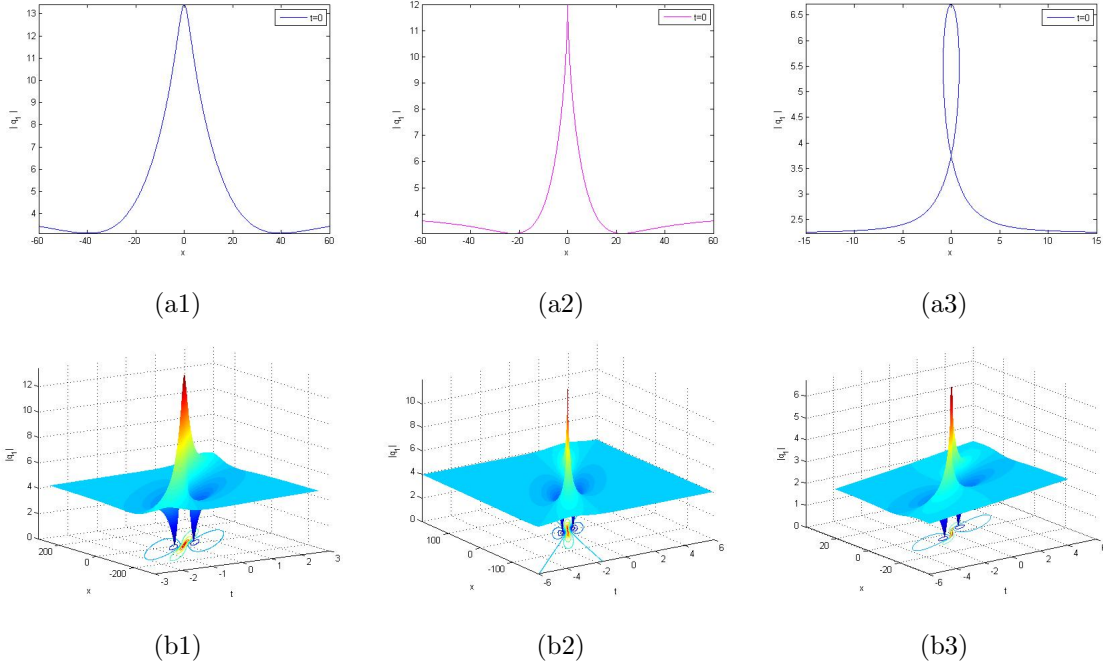


Fig. 16: Rogue wave for Eq.(7) with 2D and 3D plots, (a1)-(c1) smooth rogue wave soliton with parameter $\tau_1 = 2\sqrt{5}, \tau_2 = \sqrt{7}, k = 1$, (a2)-(c2) cusponed rogue wave soliton with parameter $\tau_1 = 4, \tau_2 = 2, k = 1$, (a3)-(c3) loop rogue wave soliton with parameter $\tau_1 = \sqrt{5}, \tau_2 = \sqrt{2}, k = 1$.

(x, t) and (y, s) . It is not possible in general to give such a relation because of too many parameters involved.

However, we can obtain the relation for the reduced case. By some tedious calculations, the single rogue wave solution can be constructed from the formular (71)-(73) by using the technique [33]

$$\begin{aligned}
q_1 &= \tau_1 e^{i\theta} \left(1 - 4 \frac{L}{M}\right), & q_2 &= \tau_2 e^{i\theta} \left(1 - 4 \frac{L}{M}\right), \\
M &= (|\tau_1|^2 - |\tau_2|^2)^2 s^2 + 4k^2(1 + k^2 y^2) + (|\tau_1|^2 - |\tau_2|^2)(4k^2 s(s - y) + 1), \\
L &= 4k^2(1 - iky) + (|\tau_1|^2 - |\tau_2|^2), \\
x &= \frac{|\tau_2|^2 - |\tau_1|^2}{2}(y + s) - 4 \frac{2k^2(2s - y) + (|\tau_1|^2 - |\tau_2|^2)s}{(|\tau_1|^2 - |\tau_2|^2)s^2 + 4k^2(1 + k^2 y^2) + (|\tau_1|^2 - |\tau_2|^2)(4k^2 s(s - y) + 1)}, \quad t = -s.
\end{aligned} \tag{77}$$

which is nothing but a rogue wave solution of Eq.(7). We emphasize that the restriction $|\tau_1| > |\tau_2|$ in (77) provides the rogue wave solution of the Eq.(7) which is localized in both space and time. A typical evolution of the rogue wave is shown in Fig.16. The peak of the rogue wave (77) at point $(x, t) = (0, 0)$ is

$$|q_1| = 3|\tau_1|, \quad |q_2| = 3|\tau_2|, \tag{78}$$

where the hole of the rogue wave (77) at point $(x, t) = (\pm \sqrt{\frac{3}{|\tau_1|^2 - |\tau_2|^2}}, \pm \frac{3\sqrt{3}}{2} \sqrt{|\tau_1|^2 - |\tau_2|^2})$ is zero. It is interesting to analyze the role of the parameter k in the rogue wave solution as well. When we increase the value of k , the width of the profile increases. Further, if $|\tau_1|^2 - |\tau_2|^2 > 12k^2$, one can obtain the smooth rogue wave solution (Figs.16(a1)); If $|\tau_1|^2 - |\tau_2|^2 = 12k^2$, one obtains the cuspon rogue wave (Figs.16(a2)); If $|\tau_1|^2 - |\tau_2|^2 < 12k^2$, one can obtain the loop rogue wave (Figs.16(a3)).

5 Conclusions

In this paper, we focus our attention on the coupled focusing-defocusing complex short pulse equation(7). By using the Hirota bilinear technique [34], the bright-bright, bright-dark, dark-dark soliton solutions, breather and rogue wave solution for the Eq.(7) are constructed. It has been shown that all these solitons have three shapes: smooth, cuspon, and loop soliton. The dynamics and asymptotic behavior of the solitons are analyzed. The interaction of the two bright-bright solitons undergo energy exchanged collision depending on the choices of the parameters. However, the interactions of bright-dark and dark-dark solitons are elastic. We have shown that the coupled focusing-defocusing complex short pulse equation admits the dark-dark soliton. Starting from the dark-dark soliton solution, we find two kinds of solutions: breather and rogue wave. The breather can be expressed as trigonometric and hyperbolic functions. The first order rational rogue wave solution is received by resorting to the Taylor series expansion coefficients. To the best of our knowledge, the dark rogue wave is found for the first time and deserves a further investigation. We have seen that there exist some difference of the property of solution between coupled nonlinear Schrödinger equations [25–33] and the coupled focusing-defocusing complex short pulse equation (7).

Acknowledgements

The work of ZNZ is supported by the National Natural Science Foundation of China under grant 11671255 and by the Ministry of Economy and Competitiveness of Spain under contract MTM2016-80276-P (AEI/FEDER,EU). We are very grateful to Prof. B.F. Feng for his many useful and constructive discussions.

References

- [1] A. Hasegawa, Y. Kodama, Solitons in Optical Communications, Oxford University Press, New York, 1995.

- [2] G.P. Agrawal, *Nonlinear Fiber Optics*, Academic, San Diego, 2001.
- [3] V. G. Makhankov, *Soliton Phenomenology*, Kluwer Academic, London, 1990.
- [4] M. J. Ablowitz, *Nonlinear Dispersive Waves: Asymptotic Analysis and Solitons*, Cambridge University Press, Cambridge, England, 2011.
- [5] M. J. Ablowitz, G. Biondini, and A. Lev Ostrovsky, Optical solitons: Perspectives and applications, *Chaos* 10, 471 (2000).
- [6] J. C. Bronski, L. D. Carr, B. Deconinck, and J. N. Kutz, Bose-Einstein condensates in standing waves: the cubic nonlinear Schrödinger equation with a periodic potential, *Phys. Rev. Lett.* 86, 1402 (2001).
- [7] E. P. Bashkin and A. V. Vagov, Instability and stratification of a two-component Bose-Einstein condensate in a trapped ultracold gas, *Phys. Rev. B* 56, 6207 (1997).
- [8] J.E. Rothenberg, Space-time focusing: breakdown of the slowly varying envelope approximation in the self-focusing of femtosecond pulses, *Opt. Lett.* 17, 1340 (1992).
- [9] T. Schäfer, C.E. Wayne, Propagation of ultra-short optical pulses in cubic nonlinear media. *Phys. D* 196, 90-105 (2004).
- [10] A. Sakovich, S. Sakovich, The short pulse equation is integrable. *J. Phys. Soc. Jpn.* 74, 239-241 (2005).
- [11] J. C. Brunelli, The bi-hamiltonian structure of the short pulse equation, *Phys. Lett. A* 353, 475-478 (2006).
- [12] Y. Matsuno, Multiloop soliton and multibreather solutions of the short pulse model equation, *J. Phys. Soc. Jpn.* 76, 084003 (2007).
- [13] Y. Matsuno, Periodic solutions of the short pulse model equation, *J. Math. Phys.* 49, 073508 (2008).
- [14] R. Beals, M. Rabelo, K. Tenenblat, Bäcklund transformations and inverse scattering solutions for some pseudo-spherical surface equations, *Stud. Appl. Math.* 81, 125-151 (1989).
- [15] E. J. Parkes, Some periodic and solitary travelling-wave solutions of the short-pulse equation, *Chaos, Solitons Fractals*, 38, 154-159 (2008).
- [16] V. K. Kuetche, T. B. Bouetou, T. C. Kofane, On two-loop soliton solution of the schäfer-wayne short-pulse equation using hirota's method and hodnett-Cmoloney approach. *J. Phys. Soc. Jpn.* 76, 024004 (2007).
- [17] B. F. Feng, K. Maruno, Y. Ohta, Integrable discretization of the short pulse equation, *J. Phys. A* 43, 085203 (2010).
- [18] B. F. Feng, J. Inoguchi, K. Kajiwara, K. Maruno, Y. Ohta, Discrete integrable systems and hodograph transformations arising from motions of discrete plane curves, *J. Phys. A* 44, 395201 (2011).
- [19] S. F. Shen, B. F. Feng, Y. Ohta, From the real and complex coupled dispersionless equations to the real and complex short pulse equations, *Stud. Appl. Math.* 136, 64 (2016).
- [20] B. F. Feng, Complex short pulse and coupled complex short pulse equations, *Phys. D* 297, 62-75 (2015).
- [21] L. Lin, B. F. Feng, Z. Zhu, Multi-soliton, multi-breather and higher order rogue wave solutions to the complex short pulse equation, *Phys. D* 327, 13-29 (2016).
- [22] B. F. Feng, L. Lin, Z. Zhu, Defocusing complex short-pulse equation and its multi-dark-soliton solution, *Phys. Rev. E* 93, 052227 (2016).
- [23] B. Guo, Y. F. Wang, Bright-dark vector soliton solutions for the coupled complex short pulse equations in nonlinear optics, *Wave Motion* 67, 47-54 (2016).
- [24] B. F. Feng, Private Communication (2016).
- [25] M. Vijayajayanthi, T. Kanna, and M. Lakshmanan, Bright-dark solitons and their collisions in mixed N-coupled nonlinear Schrödinger equations. *Phys. Rev. A* 77, 013820 (2008).
- [26] R. Radhakrishnan, M. Lakshmanan, J. Hietarinta, Inelastic collision and switching of coupled bright solitons in optical fibers, *Phys. Rev. E* 56, 2213 (1997).

- [27] T. Kanna, M. Lakshmanan, Exact soliton solutions, shape changing collisions, and partially coherent solitons in coupled nonlinear Schrödinger equations, *Phys. Rev. Lett.* 86, 5043 (2001).
- [28] T. Kanna, M. Lakshmanan, Exact soliton solutions of coupled nonlinear Schrödinger equations: shape-changing collisions, logic gates, and partially coherent solitons, *Phys. Rev. E* 67, 046617 (2003).
- [29] D. S. Wang, D. J. Zhang, and J. Yang, Integrable properties of the general coupled nonlinear Schrödinger equations *J. Math. Phys.* 51, 023510 (2010).
- [30] F. Baronio, A. Degasperis, M. Conforti, and S. Wabnitz, Solutions of the vector nonlinear Schrödinger equations: evidence for deterministic rogue waves, *Phys. Rev. Lett.* 109, 044102 (2012).
- [31] L. M. Ling, L. C. Zhao, and B. L. Guo, Darboux transformation and multi-dark soliton for N-component coupled nonlinear Schrödinger equations, *Nonlinearity*, 28, 3243-3261 (2015).
- [32] A. Mahalingam and K. Porsezian, Propagation of dark solitons in a system of coupled higher-order nonlinear Schrödinger equations, *J. Phys. A: Math. Gen.* 35, 3099 (2002).
- [33] T. Kanna and M. Lakshmanan, Exact soliton solutions of coupled nonlinear Schrödinger equations: Shape-changing collisions, logic gates, and partially coherent solitons, *Phys. Rev. E* 67, 046617 (2003).
- [34] R. Hirota, *The Direct Method in Soliton Theory*, Cambridge Univ. Press, Cambridge, 2004.
- [35] N. Vishnu Priya, M. Senthilvelan, and M. Lakshmanan, Dark solitons, breathers, and rogue wave solutions of the coupled generalized nonlinear Schrödinger equations, *Phys. Rev. E* 89, 062901 (2014).
- [36] Nail Akhmediev, Adrian Ankiewicz, and J. M. Soto-Crespo, Rogue waves and rational solutions of the nonlinear Schrödinger equation, *Phys. Rev. E* 80, 026601 (2009).
- [37] P. Dubard, P. Gaillard, C. Kleina, and V.B. Matveev, On multi-rogue wave solutions of the NLS equation and positon solutions of the KdV equation, *Eur. Phys. J. Special Topics* 185, 247-258 (2010).
- [38] B. Guo, L. Ling, Rogue wave, breathers and bright-dark-rogue solutions for the coupled Schrödinger equations, *Chin. Phys. Lett.* 28, 110202 (2011).
- [39] B. Guo, L. Ling, Q.P. Liu, Nonlinear Schrödinger equation: generalized Darboux transformation and rogue wave solutions, *Phys. Rev. E* 85, 026607 (2012).
- [40] Y. Ohta and J. Yang, General high-order rogue waves and their dynamics in the nonlinear Schrödinger equation, *Proc. R. Soc. A* 468, 1716 (2012).